MARMARA UNIVERSITY
FACULTY OF ENGINEERING

COMPUTATION OF AERODYNAMIC LOADS FOR THE AIR INTAKE OF A SUPERSONIC AIRPLANE WITH USING OPEN SOURCE CFD SOFTWARE

Barış BIÇAKÇI

GRADUATION PROJECT REPORT
Department of Mechanical Engineering

Supervisor
Prof. Dr. Emre ALPMAN

ISTANBUL, 2022

MARMARA UNIVERSITY
FACULTY OF ENGINEERING

Computation of Aerodynamic Loads for the Air Intake of a Supersonic Aircraft with Using Open Source CFD Software

by

Barış BIÇAKÇI

February 10, 2022, Istanbul

SUBMITTED TO THE DEPARTMENT OF MECHANICAL ENGINEERING IN PARTIAL FULFILLMENT OF THE REQUIREMENTS FOR THE DEGREE

OF

BACHELOR OF SCIENCE

AT

MARMARA UNIVERSITY

Signature of Author(s) ..... Barış BIÇAKÇI

Department of Mechanical Engineering

Certified By .....

Project Supervisor, Department of Mechanical Engineering

Accepted By .....

Head of the Department of Mechanical Engineering

ACKNOWLEDGEMENT

First of all, I would like to express my gratitude to my supervisor Prof. Dr. Emre ALPMAN for the valuable guidance and advice on preparing this thesis and giving me moral and material support. His guidance and advice carried me through all the stages of completion my project. He did not withhold his help and knowledge during the meetings that we held regularly every week. Thanks to this period I have considerably increased my knowledge and experience in the field of computational fluid dynamics. In this way, I found the courage to aim for graduate education in this field.

February, 2022 Barış BIÇAKÇI

CONTENTS

ACKNOWLEDGEMENT i

CONTENTS ii

ABSTRACT iv

SYMBOLS iv

ABBREVIATIONS iii

LIST OF FIGURES v

1. INTRODUCTION 10

1.1. Literature Research 11

1.1.1. Classification of Air Intakes by Compression Region 12

1.1.1.1. Internal Compression Air Intake 14

1.1.1.2. External Compression Inlet 14

1.1.1.3. Mixed Compression Inlet 15

1.1.2. Shock Wave 15

1.1.2.1. Normal Shock Wave 16

1.1.2.2. Oblique Shock Wave 17

1.1.3. Shock Wave Boundary Layer Interaction 17

1.1.4. Aerodynamic Loads 8

1.2. Scope and Outline of the Project 8

2. MATERIAL AND METHOD 20

2.1. Air Intake Geometries 21

2.1.1. Air Intake Geometry of First Case 20

2.1.2. Air Intake Geometry of Second Case 22

2.2. Mesh Generation 13

2.3. SU2 Solver Suite 26

2.3.1. Governing Equations 27

2.3.2. Turbulence Model 27

2.3.3. Convective Numerical Method 18

2.3.4. Boundary Markers 18

2.3.4.1. Boundary Markers Defined in First Case 18

2.3.4.2. Boundary Markers Defined in Second Case 29

2.4. Verification Method for First Case 20

3. RESULTS AND DISCUSSION 30
3.1. Verification of Geometry in First Case 21
3.2. Results of First Case 32
3.2.1. Contour Plots 32
3.2.2. Mach Number Values Throughout the Intake Duct 34
3.2.3. Aerodynamic Coefficients for First Case 35
3.3. Results of Second Case 26
3.3.1. Contour Plots 26
3.3.2. Aerodynamic Coefficient for Second Case 28
4. CONCLUSION AND RECOMMENDATIONS 29
4.1. Experienced Problems 30
REFERENCES 31
APPENDICES 32
APP A. Fundamental SU2 Fluid Solver Configuration File 33

ABSTRACT

Computation of Aerodynamic Loads for the Air Intake of a Supersonic Aircraft with Using Open Source CFD Software

In this project, computation of the aerodynamic loads on the air intake of the supersonic aircraft caused by the shock waves and the interaction of these shock waves with the boundary layer were performed by using a computational fluid dynamics software (CFD). For this purpose, 2-Dimensional (2D) ramp air intake of McDonnell Douglas F-15 and a supersonic air intake model with sharp cowl leading edge was examined under two specified cruise conditions and an Open-Source Software were used including Stanford University Unstructured (SU2) for flow solutions, Gmsh for mesh generation and Paraview for post-processing. Computation of aerodynamic loads was carried out separately under different flight conditions at supersonic speeds for this air intake geometry, and inferences were made by interpreting the results.

In line with this project, it was observed that the interaction between boundary layer and shock wave cause aerodynamical loads on air intake of a supersonic aircraft. These aerodynamical loads leads directly to decreasing efficiency of the engine. Computation of these loads during the design phase is therefore of great importance. The nature of the shock waves and the characteristic dynamics of supersonic viscous flows were observed and experienced in the light of the flow analyses. The high aerodynamic loads obtained and observed in the analysis results for the second case, where the Mach number was 3 as a boundary condition, within the scope of the project, helped to have an idea about the problems experienced by the air intake at high speeds. Information was obtained about the parameters that should be considered during the design phase in order for the air intake geometries to send the right quality air to the engine fan in all flight conditions.

Keywords: Computational fluid dynamics (CFD), supersonic viscous flow, aerodynamical loads, drag coefficient, air intake, variable geometry air intake, ramp angle

SYMBOLS

C_d **:** Coefficient of drag

C_l **:** Coefficient of lift

K **:** Kelvin

Re **:** Reynolds Number

ρ **:** Air Density

N **:** Newton

m **:** Meter

T **:** Temperature

ABBREVIATIONS

CFD: Computational Fluid Dynamics

SU2: Stanford University Unstructured

2D: 2 Dimensional

RANS: Reynold Average Navier Stokes

SA: Spalart Allmaras

AUSM: Advection Upstream Splitting Method

LIST OF FIGURES

PAGE

Figure 1.1 Types of intakes in supersonic aircraft 3

Figure 1.2 Types of air intake based on their location of compression region 3

Figure 1.3 Different conditions of starting of intake 4

Figure 1.4 Shock distribution along air intake duct (Aerodynamic Drag of a Two-Dimensional External Compression Inlet at Supersonic Speed - J C Esterhuyse) 6

Figure 1.5 Shock wave boundary layer interaction (AIAA Journal 51(10):2395-2409) 7

Fig 2.1 Computation of aerodynamical loads process flowchart 10

Fig 2.2 Fully open air intake of F-15 Eagle 11

Fig 2.3 Detailed sketch of the designed geometry (AIAA 2005-7357) 12

Fig 2.4 Dimension of the air intake geometry for first case 12

Fig 2.5 Geometry of air intake for second case 13

Fig 2.6 Mesh generation flow chart 13

Fig 2.7 Generated mesh in first case 15

Fig 2.8 Generated mesh in second case 15

Fig 2.9 Boundary Markers Defined in First Case 18

Fig 2.10 Boundary markers define in second case 20

Fig 2.11 Verification process of geometry in first case 20

Fig 3.1 The momentum values along the outlet 22

Fig 3.2 The mass flow rate throughout the engine fan in lb/sec (NASA Memorandum 4216) 22

Fig 3.3 Plot of Mach number contour for flow over first geometry 23

Fig 3.4 Plot of Pressure contour for flow over first geometry 24

Fig 3.5 Plot of Temperature contour for flow over first geometry 24

Fig 3.6 Mach Number values along the duct 25

Fig 3.7 Drag coefficient against number of iteration 26

Fig 3.7 Lift coefficient against number of iteration 26

Fig 3.8 Plot of Mach number contour for flow over first geometry 27

Fig 3.9 Velocity vector for flow 28

Fig 3.10 Plot of Temperature Contour for flow over second case 28

Fig 3.11 Drag Coefficient against number of iterations 29

Fig 3.12 Lift Coefficient against number of iterations 29

LIST OF TABLES

PAGE

Table 2.1 Solver Suits and Boundary Conditions for two different analysis cases **.....16**

1. INTRODUCTION

Gas turbine engines, which are also called jet engines are the most popular engines that are used in modern passenger and military aircraft for power. There are several different types of gas turbine engines but all turbine engines have some parts in common. All jet engines have an air intake to bring free stream air into the engine. These air intakes are designed to provide a relatively distortion-free flow of air, in the required quantity, towards the fan of the compressor. In the aircraft the inlet design is one of the most important parameters to bringing the air to suitable conditions for the rest of the engine. To be able to provide these suitable conditions a uniform and steady airflow is necessary to avoid compressor stall (airflow tends to stop or reverse direction of flow) and excessive internal engine temperatures in the turbine section. Ordinarily, the air-inlet duct is considered an airframe part and not a part of the engine. However, the duct is very important to the overall performance and ability of the engine to produce an optimum amount of thrust.

Bringing the air to suitable conditions for the rest of the engine is more critical in determining engine and aircraft performance, especially in aircraft that cruising at supersonic speeds. For an aircraft flying faster than Mach 1 (beyond the speed of sound) the air entering the intake is flow supersonically as well. But there is no turbojet engine compressor is capable of handling supersonic air flow because of the shockwaves. Except for scramjet with supersonic combustion chamber. For this purpose, the duty of an appropriate engine inlet is to slow incoming air to subsonic speeds before it passes through the engine by establishing a shock system including series of oblique and normal shock with minimal losses. Achieving these purposes with minimal losses requires complex engineering solution.

While the shock waves that occurring in the intake duct, make reflections, they interact with the boundary layer formed due to the no slip condition in the areas close to the surfaces. Depending on the flight conditions, these interactions of shock waves with the boundary layer can cause thickening of the boundary layer, reverse flow along the air intake duct and even hammer shock. These situations with the potential to cause serious damage to aircraft should be considered from the beginning of the vehicle's preliminary design process and necessary analyzes should be made to create an appropriate air intake duct to withstand aerodynamic loads.

An air intake design is often dependent on the conditions in which the aircraft will operate and conditions such as take-off weight.

In previous years, data on engine air intake design was only available through wind tunnel tests. Damages caused by fluctuations and loads in the air intake duct could only be obtained through post-flight inspections or prototype tests. Experimental analysis and solution of such problems are difficult and often lead to costly results. Recently, the CFD method has become more applicable and widespread for the analysis and resolution of such situations. CFD methods often provide great savings in terms of cost, time and resources. In addition, the simulations made with CFD methods and the wind tunnel facilities that have developed over time have made it very easy to understand the physics of internal flow. Today, in addition to commercial CFD software, open source CFD software has started to become widespread by many companies considering their financial advantages. In this study, 2D analysis of the air intake geometry of the McDonnell Douglas F-15 Eagle aircraft and supersonic air intake model with sharp cowl leading edge were performed using SU2, an open-source software developed by the Stanford University.

1.1. Literature Research

The performance of an air intake is playing important role on the performance and efficiency of aircraft engine as well. The performance parameters are related to three basic characteristics. They are the magnitude and quality of the pressure recovery, the capture area ratio (or mass-flow ratio), and the total drag of the diffuser. The over-all worth of a diffuser must always be determined by simultaneously assessing all three characteristics since the gain in one is often achieved at the expense of another. It should also be borne in mind that the most serious aspect of the engine-inlet problem is concerned with off-design operation: none of the characteristics should deteriorate rapidly under conditions of overspeed or under speed or at angles of attack. In actual vehicles many compromises have to be made in order to achieve an acceptable performance throughout the variations of flight Mach number, angles of attack, and sideslip as well as variations in the properties of the atmosphere. A variable-geometry inlet often achieves a better compromise than may be possible with a fixed-geometry diffuser. For this reason, air intakes with variable angle ramps that can adapt to different flight conditions are used in a few aircraft today. There are many different air intake geometries designed to serve this and other different purposes.

In supersonic aircrafts air intakes can be categorized by their;

- Installation Position
- Flow Compression Region
- Flow Dimensions

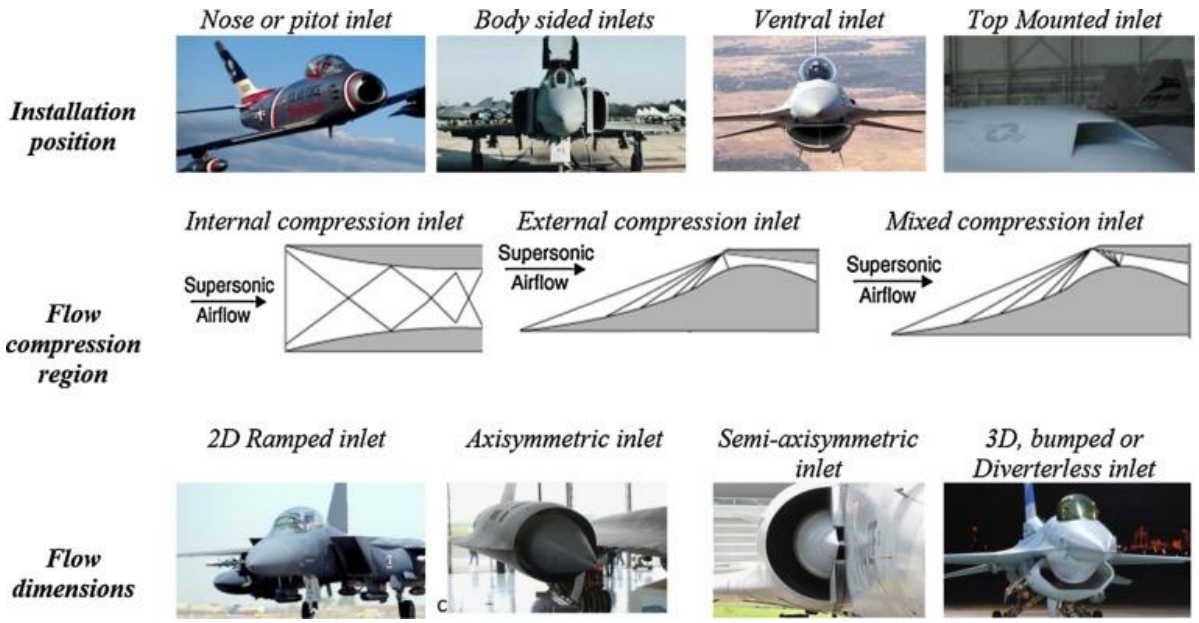

Figure 1.1 Types of intakes in supersonic aircraft

1.1.1. Classification of Air Intakes by Compression Region

Supersonic inlets based on the location of compression region, are classified into three basic types of;

- Internal compression,
- External compression,
- Mixed compression inlets.

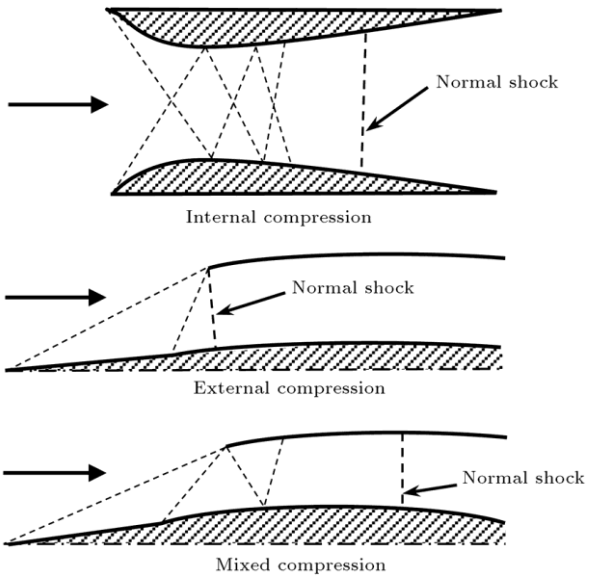

Figure 1.2 Types of air intake based on their location of compression region

1.1.1.1. Internal Compression Air Intake

In internal compression inlet, compression is achieved by a series of oblique shock waves in the internal part of the inlet following by a weak normal shock downstream of the throat. In some types of supersonic inlet, establishing a shock system with minimal losses is not easy. The process of establishing a stable shock system is referred to as starting of an inlet. Before the inlet operates in a supersonic flow, it must pass through the subsonic flow regime. This parameter sometimes results in not starting problem. Let us consider the Mach number which is slightly less than the design Mach number of engine. In this case the shock will get attached to the leading edge of the inlet. This is not desirable because pressure losses occur. Spillage is minimal in this case because the capture area is equal to the intake entry area. But the stagnation pressure losses still persist. If we consider the Mach number which is slightly more than design Mach number. The shock is now move into the intake. This is again not desirable. If we consider the Mach number equal to Design Mach Number. The normal shock waves which is weak shock moves slightly upstream and attains a stable position at just after the throat. This is the ideal case that one would like to have before the inlet is set to have been started. Pressure losses across the shock is minimal.

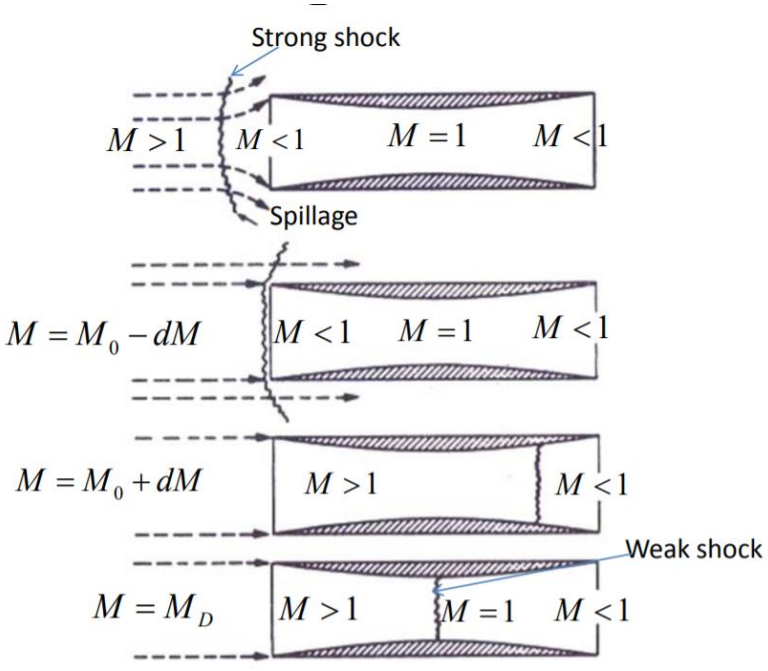

Figure 1.3 Different conditions of starting of intake

1.1.1.2.External Compression Inlet

In the external compression inlet compression region of shockwaves involves in outside geometry of inlet.

1.1.1.3.Mixed Compression Inlet

The mixed compression inlet achieves a portion of compression through one or more external oblique shock waves on the spike. The rest of compression occurs in the internal part of the inlet by reflected oblique shocks and the weak normal shock downstream of the throat.

1.1.2. Shock Wave

In physics, a shock wave or shock, is a type of propagating disturbance that moves faster than the local speed of sound in the medium. Like an ordinary wave, a shock wave carries energy and can propagate through a medium but is characterized by an abrupt, nearly discontinuous, change in pressure, temperature, and density of the medium. For the purpose of comparison, in supersonic flows, additional increased expansion may be achieved through an expansion fan, also known as a Prandtl–Meyer expansion fan. The accompanying expansion wave may approach and eventually collide and recombine with the shock wave, creating a process of destructive interference. The sonic boom associated with the passage of a supersonic aircraft is a type of sound wave produced by constructive interference.

The most basic feature of the shock wave is that it creates discontinuities in the pressure, density and velocity vector field during flow. As a result of the shock wave, the total pressure and velocity decrease, and the static pressure and density rise. Shock waves are adiabatic and irreversible, so they create a significant increase in entropy. Air vehicles consume incredible fuel at supersonic speeds, as the total pressure losses increase the drag force.

Shock waves play an important role in the air intakes of aircraft traveling at supersonic speeds, as they are effective in reducing the velocity of the flow. The air inlets are designed to supply the air they take at supersonic speeds towards the compressor's fan with the help of a series of shock waves and in the required amount relatively distortion-free at subsonic speeds. For this purpose, some air intakes have movable ramps. These ramps act under certain conditions at certain moments of flight and cause changes in the geometry of the air intake. As a result of these changes, shock waves are created in the optimum number and shape, and it is ensured that the air going to the engine is brought to the desired conditions. The ramp sits at an acute angle to deflect the intake air from the longitudinal direction. At supersonic flight speeds, the deflection of the air stream creates a number of oblique shock waves at each change of gradient along at the ramp. Air crossing each shock wave suddenly slows to a lower Mach number, thus increasing pressure. After this series of oblique shock,

in the throat of intake duct normal shock wave occurs and flow become stable and subsonic (Figure 1.4).

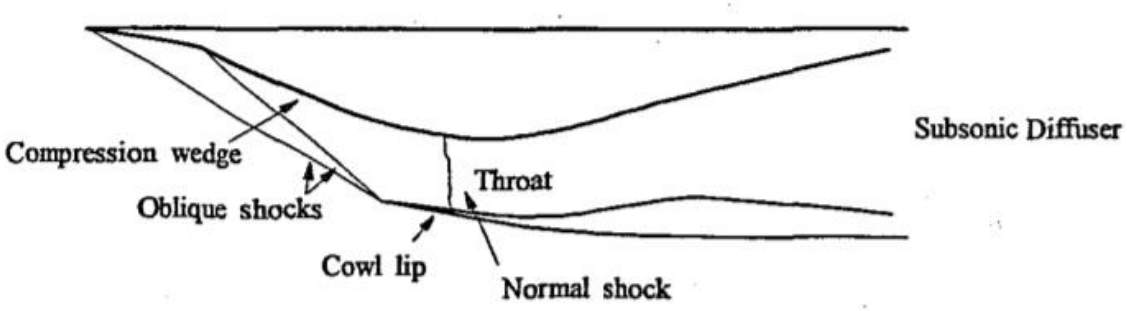

Figure 1.4 Shock distribution along air intake duct (Aerodynamic Drag of a Two-Dimensional External Compression Inlet at Supersonic Speed - J C Esterhuyse)

Ideally, the first oblique shock wave should intercept the air intake lip, thus avoiding air spillage and pre-entry drag on the outer boundary of the deflected stream tube. For a fixed geometry intake at zero incidence, this condition can only be achieved at one particular flight Mach number, because the angle of the shock wave becomes more acute with increasing aircraft speed.

1.1.2.1.Normal Shock Wave

It is an adiabatic wave and is positioned perpendicular to the velocity vector. After the normal shock wave of the flow, the velocity unit vector remains stable, but there is an incredible increase in entropy with accompanying total pressure loss. Since the entropy will have to increase, the shock wave is only seen in supersonic flows and after the shock the flow goes into the subsonic regime. It occurs between two points on the temperature-entropy diagram where the graphs of the Rayleigh and Fanno flow intersect. Rayleigh and Fanno are two types of non-isentropic flows. Fanno adiabatic, frictional; Rayleigh is frictionless and non-adiabatic flow. Using Rayleigh and Fanno, continuity and ideal gas equations, the post-shock Mach number, total pressure loss, and static pressure increase can be calculated depending on the pre-shock Mach number.

On the other hand, serious total pressure losses do not occur at low Mach number flows. For example, in a normal shock wave that will occur at a flow of 1.2 Mach, the total pressure loss is 0.72%, while at a flow of 1.4 Mach it is 4.2%, and at Mach 5 it is 93.87%. There is no boundary layer that will not be affected by the static pressure increase that this will bring, and the flow is separated.

In transonic flights, on the other hand, by changing the geometry of the wing, the velocity gradient is increased more in the region close to the trailing edge. Although it causes loss of subsonic performance, pressure losses will be minimized due to the reduced local Mach number in the transonic regime. In addition, the risk of flow separation due to the decreasing

shock intensity is eliminated.

1.1.2.2.Oblique Shock Wave

An oblique shock wave, unlike a normal shock, is inclined with respect to the upstream flow direction. It will occur when a supersonic flow encounters a corner that effectively turns the flow into itself and compresses. The upstream streamlines are uniformly deflected after the shock wave. The most common way to produce an oblique shock wave is to place a wedge into supersonic, compressible flow. Similar to a normal shock wave, the oblique shock wave consists of a very thin region across which nearly discontinuous changes in the thermodynamic properties of a gas occur. While the upstream and downstream flow directions are unchanged across a normal shock, they are different for flow across an oblique shock wave.

1.1.3. Shock Wave Boundary Layer Interaction

When an aircraft is in supersonic flight, the air entering the inlet of its propulsive system is, by definition, going faster than the speed of sound. Because of this, shockwaves are generated in the flow that take the air from a high speed and low pressure to a lower speed and higher pressure. At the same time, as air enters the inlet, there is an area very close to the walls where the velocity of the air goes from the supersonic freestream velocity to zero at the wall surface. This area is called a boundary layer and it is a major source of friction, heat, and losses in the system. As you get closer to the Wall surface velocity drops from its freestream value to zero. This means the flow along the wall is subsonic and cannot sustain the pressure discontinuities associated with shockwaves. Therefore, interactions involving shockwaves and boundary layers might cause recirculation zones which cause larger zones of influence upstream and downstream of the shockwave impingement point.

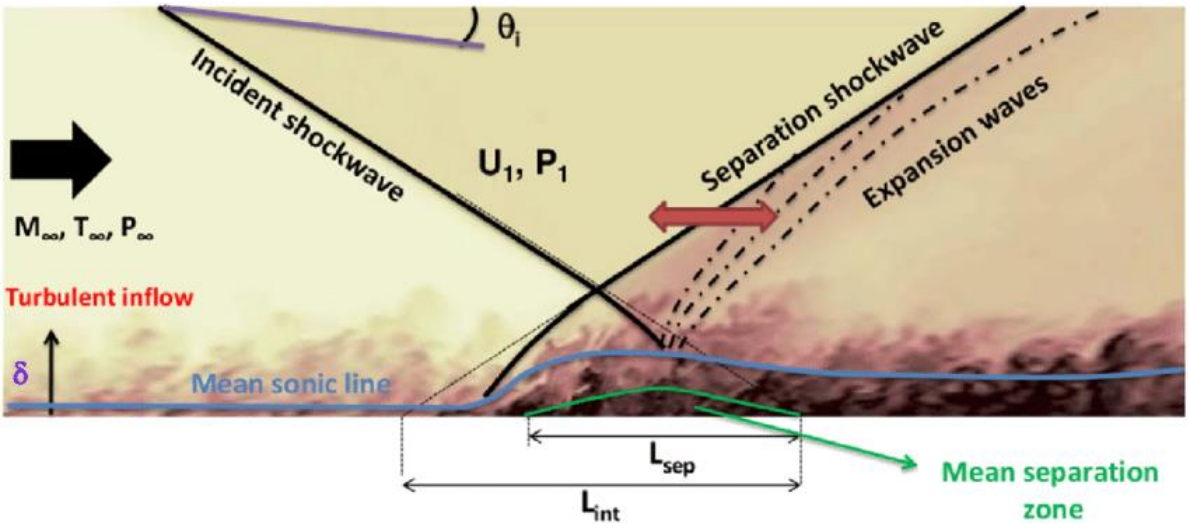

Figure 1.5 Shock wave boundary layer interaction (AIAA Journal 51(10):2395-2409)

1.1.4. Aerodynamic Loads

During cruise, an airplane and its air intake structure are subjected to two types of loads: inertia and aerodynamics. Aerodynamic loads result from the effects of the distribution of compressive forces acting on the exterior surface of the plane parts. These loads cannot be measured directly during the flight; however, they are usually determined using numerical methods.

Drag force is the resistance force caused by the motion of a body through a fluid. A drag force acts opposite to the direction of the oncoming flow velocity. This is the relative velocity between the body and the fluid. The drag force, which is an inevitable consequence of an object moving in a fluid, is an aerodynamic load that negatively affects aircraft and air intake. The drag caused by the air intake has a significant influence on the amount of net thrust available to fulfill the flight requirements. The total drag force of the inlet consists of different drag contributing components characterized by a specific geometric shape and flight requirements. That is why it has a crucial importance to establish an accurate computation and figure for the drag force of the intake to be able to increase thrust and efficiency of intake and engine.

In this report drag coefficients on two different supersonic 2D air intake with ramp was computed under specified flight conditions.

1.2. Scope and Outline of the Project

The intake drag can be considered as both part of the overall aircraft drag and the component drag since each component on the aircraft increases the drag by creating resistance against the flow. The installation of the intake on the air frame must ensure minimum drag. The shape component of drag is minimized by sizing the intake to the desired air flow rate of the engine and optimizing the shape to reduce the drag coefficient. The only way to computation of the drag and take action against possible critical situations is possible with post-flight inspection. For this reason, calculation of aerodynamic loads using computational fluid dynamics method offers low-cost solutions at the design phase.

Therefore, this project mainly focuses on computation of drag which is an aerodynamic load, acting on a supersonic air intake while familiarizing with an open source CFD software SU2.

Open-source software has started to become widespread and supported by users day by day

due to their targeting of sharing and development and not demanding any money from the user. Although Su2 does not offer a user-friendly interface, it was chosen in this project in order to keep up with the developments and to develop myself in more detail with the CFD method.

To perform computation of aerodynamic loads, in the first case two-dimensional, mixed compression, two-ramp supersonic inlet of F-15 Eagle model was chosen. The air intake of the F-15 Eagle aircraft was chosen because its simple geometry is suitable for a two-dimensional CFD study. However, air intakes of aircraft such as the Concorde and F-15 Eagle are called variable geometry air intakes. This is due to these aircraft have air intake control system to be able to satisfy the basic requirements to supply the correct amount of air at a high efficiency and in a form that is acceptable to the engines at all flight and engine operating conditions of the aircraft. The air intake control system adjusts the geometry of the air intake to the flight conditions by changing the angles of the ramps in the air intakes depending on the flight conditions. In this study, due to the fact that the F-15 Eagle air intake has different geometries at different stages of flight and the air intake dimensions of this military jet cannot be found clearly in the literature, the optimized geometry from the optimization study performed on the 2D supersonic air intake published by the American Institute of Aeronautics and Astronautics in order to maximize the total pressure recovery, taken as referenced. Thanks to the reference geometry and the article, the analysis results obtained while familiarizing with the SU2 could be compared and the accuracy of the results was ensured. By using the reference geometry and the images of the F-15 Eagle aircraft, a geometry close to the air intake geometry of the F-15 Eagle aircraft was obtained. The ramp angles of the air intake geometry were determined as the reference ramp angles in the geometry which optimized for pressure recovery. In the reference study, the ramp angles were designed at the cruise conditions of flight Mach number 2.2 and flight altitude 55,000 feet. Therefore, the calculation of the aerodynamic loads on the air intake geometry determined in the first case was planned to be carried out for this cruise conditions, the results obtained could only be confirmed for one boundary condition. After the flow solution, results are confirmed by the using flight data of F100 engine from ‘’NASA Technical Memorandum 4216’’ which is a study about a preliminary evaluation of an F100 engine parameter estimation process using flight data. Since McDonnell Douglas F-15 Eagle powered by two F100 engine and the mass flow rate requirement of engine is the same during cruise, the mass flow rate data from this article was compared.

For the second case another air intake geometry with sharp cowl leading edge was examined. For this second case, again the ramp angle of the air intake and boundary

conditions was determining by taking the study about ‘’Alterations of Cowl Lip for the Improvement of Supersonic-Intake Performance’’ as reference. In the reference study, the ramp angles were designed at the cruise conditions of flight Mach number 3 together with freestream static pressure of 15 kPa and static temperature of 135 K. Therefore, the calculation of the aerodynamic loads on the air intake geometry determined in the second case was planned to be carried out for this cruise conditions.

Going back to the beginning of the cycle of the project, the creation of geometry and mesh generation done by GMSH which has both GUI and Python based script for mesh generation and supports direct output to the SU2 format. Finally, PARAVIEW was used for post-processing the numerical solution. These processes will be detailed later.

2. MATERIAL AND METHOD

The present study undertakes the computation of a supersonic two different 2D ramp air intake in which numerical tools are utilized. In this chapter theoretical background and used method of flow solution and the tools that used during this process are clarified. Firstly, governing equations, solution procedures and boundary conditions are explained in detail. After that, meshing process is presented. Details of the whole process are presented also by following computation aerodynamic loads process flowchart (Fig 2.1).

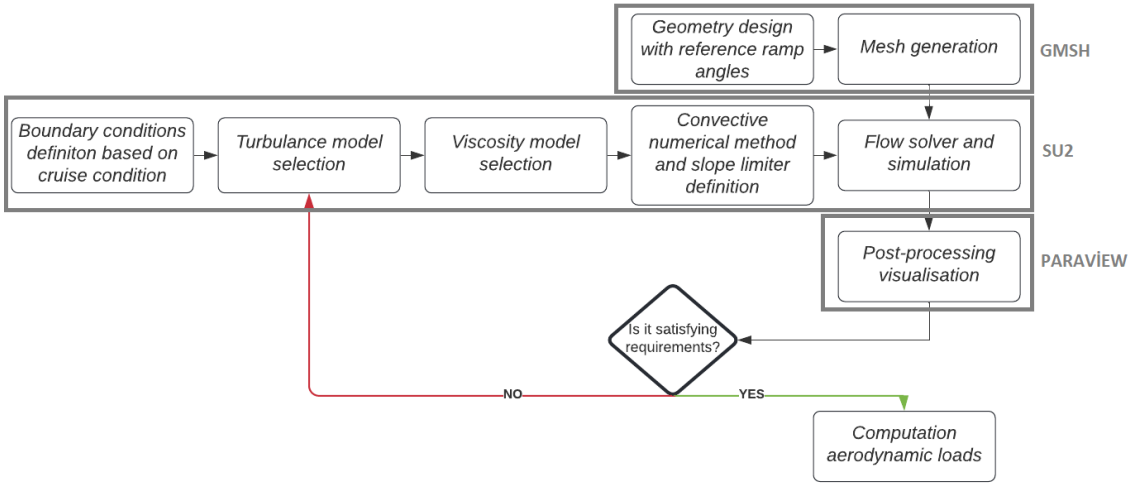

Fig 2.1 Computation of aerodynamical loads process flowchart

2.1. Air Intake Geometries

In this project, two different geometries were determined for flow solutions. Different ways have been followed to model these geometries and determine their dimensions. In both air intake geometries, there are 2 variable ramps that change depending on the flight conditions and boundary conditions. Angles of these ramps managed by the air intake control system are identical for every cruise condition to be able to satisfy the basic requirements to supply the correct amount of air at a high efficiency and in a form that is acceptable to the engines at all flight and engine operating conditions of the aircraft. Therefore, by making a literature review, studies that have been carried out before and in which the ramp angles of the air intakes are optimized for certain flight conditions are taken as reference. Another reason for reference is that any measure of the air intake geometry of the F-15 Eagle military jet could not be reached.

2.1.1. Air Intake Geometry of First Case

As mentioned before, for the first case, the geometry and the ramp angle of air intake were determined based on the referenced study and the intake geometry of F-15 Eagle. Afterwards, the photographs of the F-15 eagle aircraft were examined and the final geometry was obtained by optimizing the ramp angles in the reference geometry to remain constant. The following figures are shown the referenced geometry and actual air intake of F-15 Eagle.

Fig 2.2 Fully open air intake of F-15 Eagle

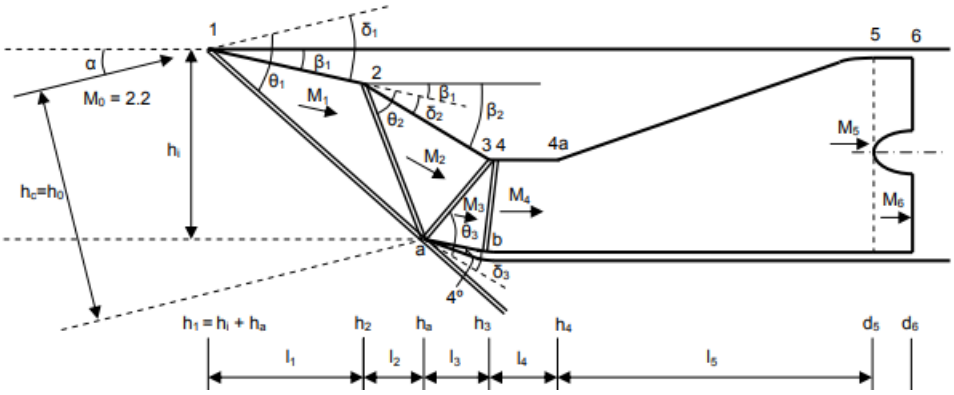

Fig 2.3 Detailed sketch of the designed geometry (AIAA 2005-7357)

The sketch of the air intake geometry in Fig 2.3 were design to be able to obtain optimum shock wave during cruise at flight Mach number of 2.2 and altitude of 55000 feet. The oblique shock waves from the two external ramps intersect at the cowl leading edge, and the third oblique shock reflects upward to intersect the junction of the final ramp and the throat section. This shock system obtained by proper ramp angle, provide to decelerate the supersonic flow to a subsonic number and the diffuser provide further reduce the flow speed to the engine face entry speed. By this way, total pressure recovery can be maximized.

In order to obtain this shock system and achieve the actual air intake geometry of the F-15 Eagle, the following geometry shown in Fig 2.4 has been designed for first case.

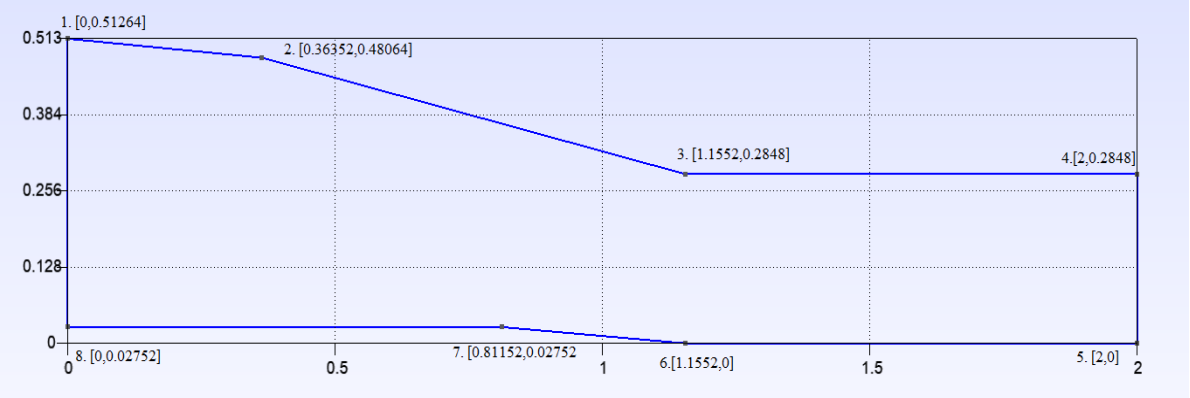

Fig 2.4 Dimension of the air intake geometry for first case

2.1.2. Air Intake Geometry of Second Case

As mentioned before, for the second geometry a different air intake geometry with sharp cowl leading edge was examined. In this case, the geometry of air intake also has 2 ramps. For this geometry, the air intake of Scramjet and the study published by Journal of Applied Fluid Mechanics were referenced. The following geometry shown in Fig 2.5 has been examined for second case.

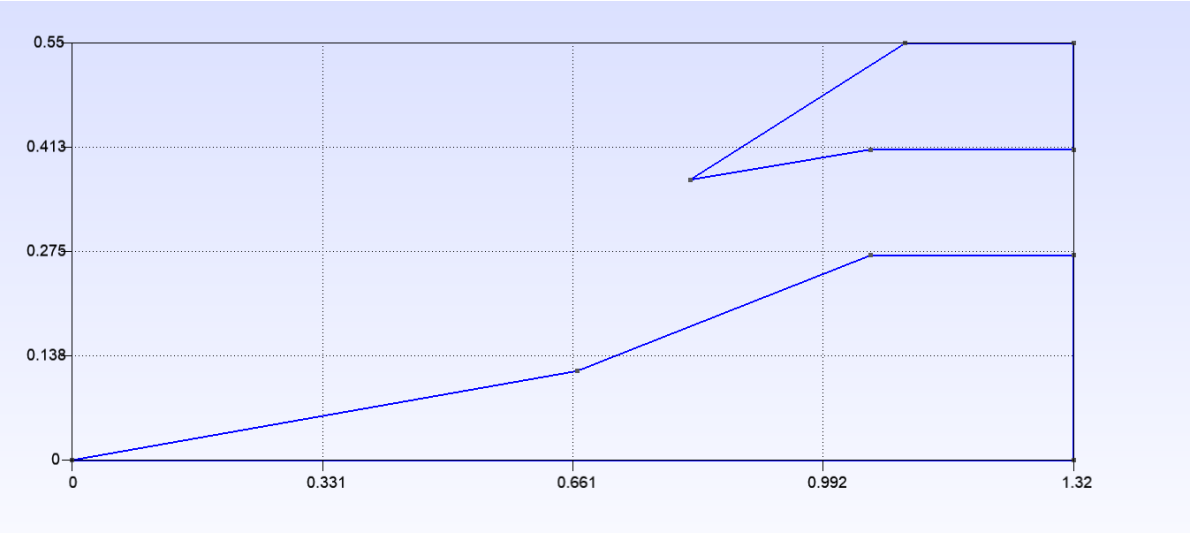

Fig 2.5 Geometry of air intake for second case

2.2. Mesh Generation

Gmsh was utilized for 2D drawing and modeling of air intake geometry and mesh generation. Although Gmsh has not a user-friendly interface, it was used since the strict requirements of SU2 for generating a readable file for SU2 can be met by using Gmsh. Gmsh is an open-source code with dual features of both a GUI and Python based script. By using Gmsh, generated mesh can be exported as .su2 file. Gmsh has four modules which are geometry, mesh, solver and post-processing. Gmsh can be used by three ways as following;

- Through the GUI
- Through the dedicated .geo language
- Through the C++, C and Python

In the present study, GMSH is used with combination of GUI and .geo dedicated language code. Details of the mesh generation process are presented by following flowchart in Fig 2.6.

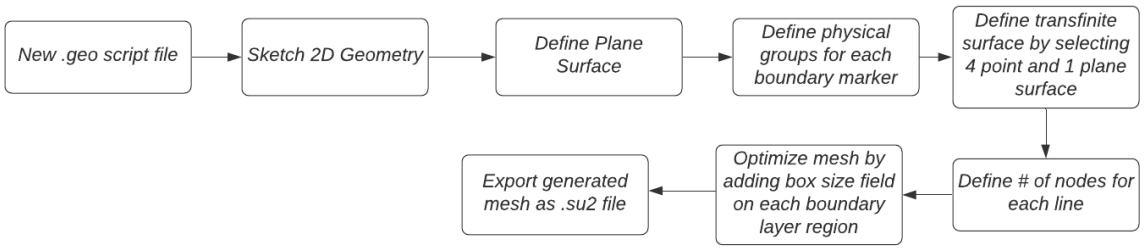

Fig 2.6 Mesh generation flow chart

Some problems encountered during mesh generation. The boundary layer is the region where viscous effects are dominant. In the both two cases where flow analysis is carried, the interaction of the boundary layer and shock waves is of great importance for the accuracy of the analysis. For this reason, it is very important to make a fine mesh for the boundary layer while mesh generation. However, mesh generation for the boundary layer could not be performed using the size field option of Gmsh. Instead, box meshing was done with the size field option of GMSH on the areas with wall boundary markers in thicknesses approximately equal to the thickness of the boundary layer. This process done for every wall section of the geometry for both case by adding following script to .geo file according to their coordinate;

```
//+
Field[1] = Box;
//+
Field[1].Thickness = 0.5;
//+
Field[1].VIn = 0.05;
//+
Field[1].VOut = 1;
//+
Field[1].XMax =  %Maximum X coordinate of the box;
//+
Field[1].XMin = %Minimum X coordinate of the box;
//+
Field[1].YMax = %Maximum Y coordinate of the box;
//+
Field[1].YMin = %Minimum Y coordinate of the box;
//+
Background Field = 1;
```

For the rest of the domain, structured transfinite mesh were generated. Since the computational domain for both cases are small, all domain were meshed with small elements without considering computation time. Fig 2.7 and Fig 2.8 shown the mesh properties for each case separately.

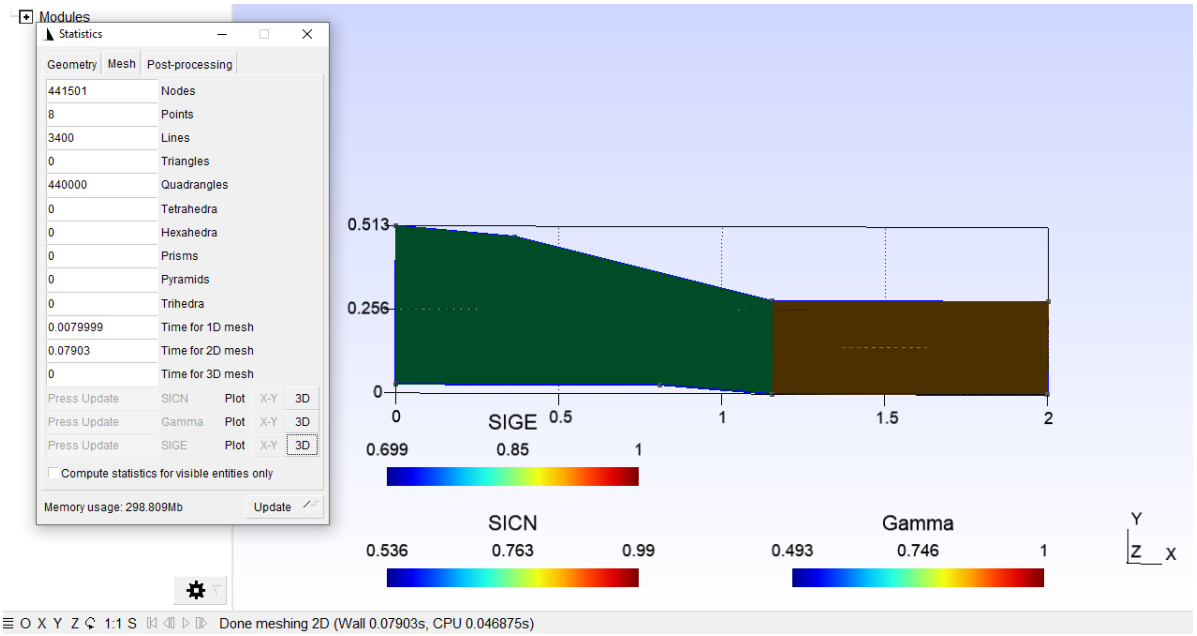

Fig 2.7 Generated mesh in first case

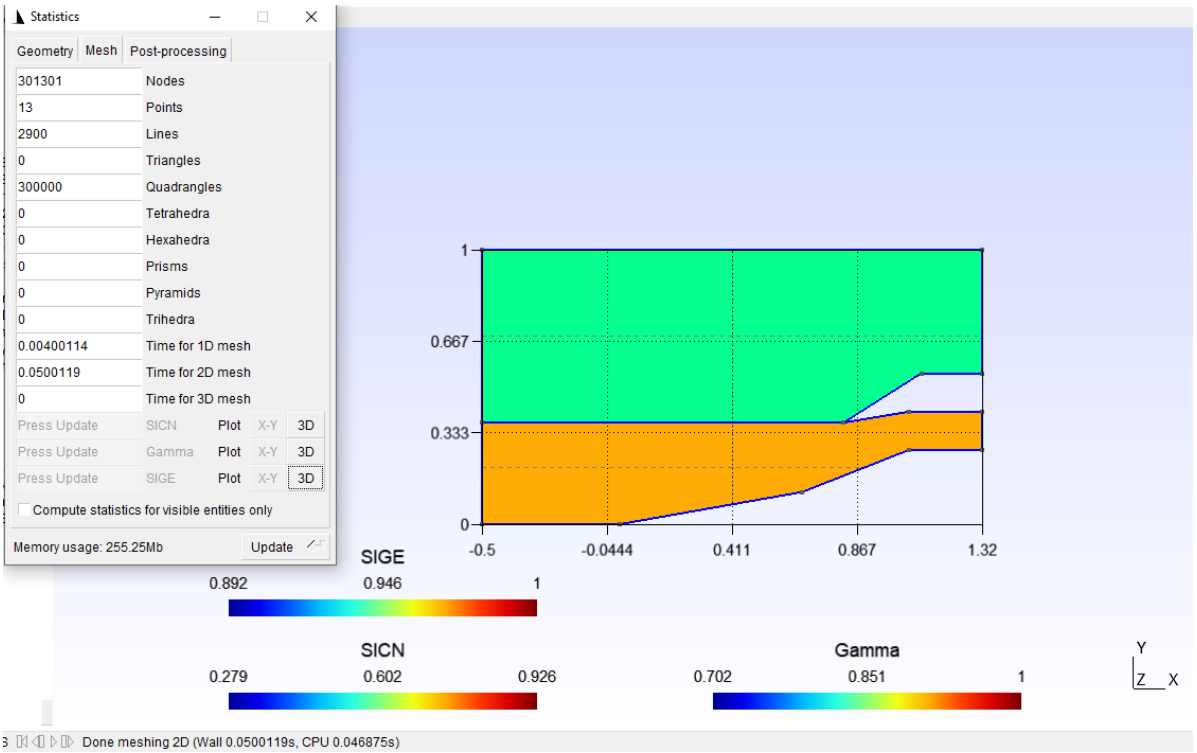

Fig 2.8 Generated mesh in second case

2.3. SU2 Solver Suite

Stanford University Unstructured (SU2) flow solver which is an open-source software collection, is being developed to solve complex, multi-physics analysis and optimization tasks using arbitrary unstructured meshes, and it has been designed so that it is easily extensible for the solution of Partial Differential Equation-based (PDE) problems not directly envisioned by the authors. At its core, SU2 is an open-source collection of C++ software tools to discretize and solve problems described by PDEs and is able to solve PDE-constrained optimization problems, including optimal shape design. Although the toolset has been designed with CFD and aerodynamic shape optimization, it has also been extended to treat other sets of governing equations including potential flow, electrodynamics, chemically reacting flows, and several others. Capabilities for computational analysis and optimization have improved considerably over day by day. In this study SU2 was used for flow solver to perform flow solutions. Fundamental solver suit parameters and boundary conditions for both cases are presented in the Table 1. Considering the cruise conditions, boundary conditions that required to define in configuration file, such as pressure, temperature of freestream, flow Reynolds number were computed.

Table 1.1. Solver Suits and Boundary Conditions for two different analysis cases

SU2 Solver Suite	First Case	Second Case
Physical Governing Eqn.	RANS	RANS
Turbulence Model	SA	SA
Fluid Model	Standard Air	Standard Air
Viscosity Model	Sutherland	Sutherland
Numerical Method for Spatial Gradients	Green Gauss	Green Gauss
Convective Numerical Method	AUSM	ROE
Slope Limiter Flow	Van Albada Edge	Van Albada Edge
Convergence Parameter	RMS_Density	RMS_Density
Flight Mach Number	2.2	3

Flight Altitude (m)	16764	-
Freestream Temperature (K)	216.667	135
Freestream Pressure (Pa)	9183.82	15000

2.3.1. Governing Equations

In the first place since it is known that the solution of flow in a supersonic air intake will deal with shock waves and their interactions with the boundary layer, the flow over supersonic air intake considered as viscous and compressible. In this way, more accurate results are obtained. In the light of this considerations Reynolds-averaged- Navier-Stokes equations are solved using SU2 with the finite volume method for both cases.
Navier-Stokes equations expressed in differential for as below Equation (1).

$$\frac{\delta U}{\delta t} + \nabla . \bar{F}^{c}(U) - \nabla . \bar{F}^{v}(U, \nabla U) - S = 0 \qquad (1)$$

To include the turbulence factor, Reynolds decomposition is performed in which the instantaneous quantity of the variables due to the turbulence are divided into their time-averaged and fluctuating quantities. Variables defined in the Navier-Stokes equation are replaced with the time-averaged and fluctuating quantities of the variables and due to fluctuation terms in the velocity, an additional stress term appears to be solved in the momentum equations called the Reynolds stress. To solve the Reynolds stresses, a turbulence model is used and the system of equations is called as Reynolds-averaged Navier-Stokes equations. RANS equations are widely used for compressible and turbulent flows. In SU2 differential form of the Navier-Stokes equation is converted to integral form by using the Reynolds Transport theorem and the integral form of the Navier-Stokes equations is given in Equation (2).

$$\int_{\Omega i} \frac{\partial U}{\partial t} d\Omega + \sum_{j \in N(i)} \left(\bar{F}_{ij}^{c} + \bar{F}_{ij}^{v} \right) \Delta S_{ij} - Q|\Omega i| = 0 \qquad (2)$$

Convective and viscous fluxes are projected into local and normal directions of edge and ΔS_{ij} is the area of the associated face with the edge 'ij'. The term $Q|\Omega i|$ is the volume of the dual control volume and N(i) is the set of neighboring nodes to node 'I'.

2.3.2. Turbulence Model

As it mentioned before, since the solution of flow in a supersonic air intake will deal with shock waves and their interactions with the boundary layer, The Spalart-Allmaras (SA) turbulence model which is one equation turbulence model was selected for both analysis cases in this project. The SA model is one of the most common and widely used turbulence model in aerodynamic solution. This model demonstrates acceptable results for the solution of the adverse pressure gradient and boundary layer. Since SA is a one equation model, the computation time is less and the solution converges faster compared to two equation models.

2.3.3. Convective Numerical Method

The convective and viscous fluxes are evaluated at the midpoint of an edge. SU2 has different schemes for convective flux discretization which are Jameson Schmidt Turkel (JST), Roe, Advection Upstream Splitting Method (AUSM), HLLC, and Roe-Turkel.
In the first case AUSM which is a numerical flux function is used for solving a general system of conservation equations. The AUSM has many features, such as accurate capturing of shock and contact discontinuities, entropy-satisfying solution, uniform accuracy and convergence rate for all Mach numbers.
In the second case since the outside domain of the air intake was also computed, the ROE scheme was selected as convective numerical method.

2.3.4. Boundary Markers

2.3.4.1. Boundary Markers Defined in First Case

To define the boundary marker there are several options in SU2. In first case 4 different boundary marker were used. These markers are illustrated in Fig 2.9.

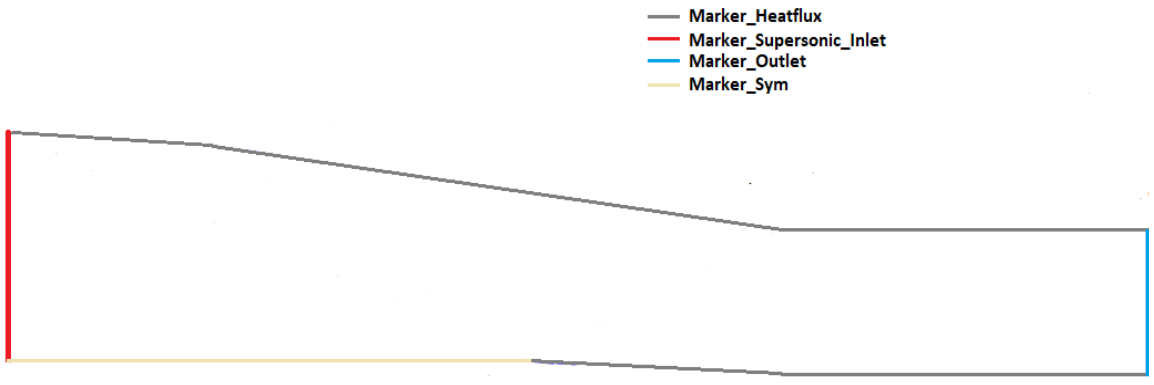

Fig 2.9 Boundary Markers Defined in First Case

Since the air intake model has an asymmetrical geometry, it was necessary to define a boundary mark at the bottom of the air intake from the inlet to the lower wall. For this boundary marker, it was first considered to define a farfield boundary marker. However, due to the results obtained after the flow solution, the fact about boundary mark being close to the inlet and wall boundary marks and the outside region was not interested in the domain to be analyzed, the farfield boundary marker was abandoned. Instead, other studies with the same situation were reviewed and it was decided to define a symmetry boundary marker. Then the rest of the boundary markers defined as follow;

- Marker_Supersonic_Inlet: This boundary marker defined for the inlet. In SU2, to define this marker, its required to specify temperature, static pressure and velocity values for each direction. These values are defined as the same value of free-stream by considering cruise conditions for each case.
- Marker_Outlet: This boundary marker defined for the exit of air intake. To define this marker a back pressure value for outlet was set. However the examined flow conditions are supersonic and all characteristics are outgoing, meaning that no information about the exit conditions is required.Since propagation of information in this supersonic flow make it unnecessary information the outlet back pressure value was set to the approximate value.
- Marker_Heatflux: This marker defined for all the walls of air intake. The heat-flux values were set as 0 to make marker pretend as solid wall.
- Marker_Monitoring: By using this marker and defining this marker as wall of the air intake, calculation of aerodynamic coefficients such as Cd and Cl on the wall is provided.

2.3.4.2.Boundary Markers Defined in Second Case

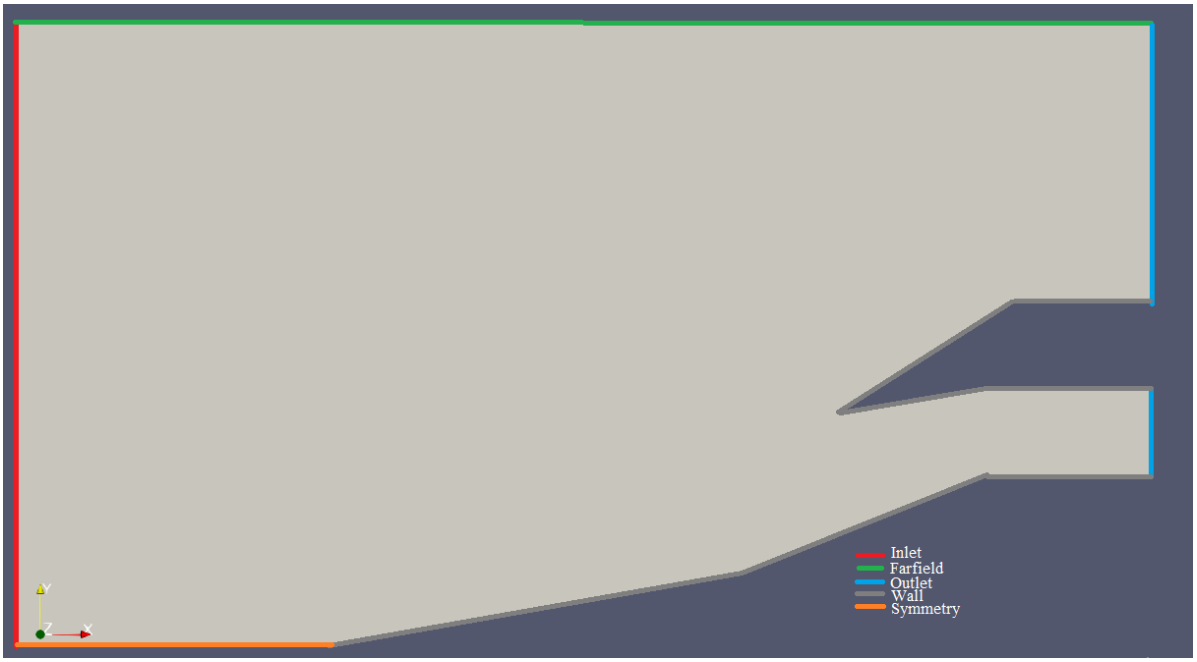

Fig 2.10 Boundary markers define in second case

As illustrated in Fig 2.10 for the second case 5 different boundary marker were used. For this case to define a marker for the upside of the domain, Farfield marker was selected. The rest of the boundary markers are defined as in the first case.

2.4. Verification Method for First Case

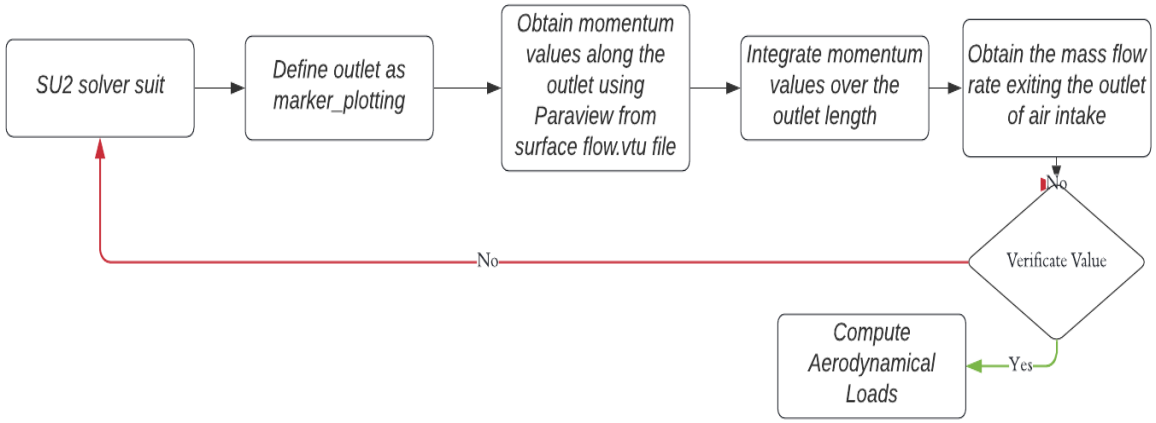

Fig 2.11 Verification process of geometry in first case

As mentioned before, the geometry designed for the first case were optimized by considering references geometries. Therefore, a verification of flow solution results needed to be made. For this purpose, the flight data taken from NASA Technical Memorandum 4216 were used. In this article published by Nasa, the flight data of F-100 engine at flight Mach number 0.9 and flight altitude 9000 meter were given. Although the flight conditions

in the first case are not the same as the flight conditions in this article, it is known that the mass flow rate value required by the engine throughout the flight is constant in the light of the information obtained from the literature research. Therefore, to calculate the mass flow rate value by integrating the momentum values, the outlet is selected as Marker_Plotting in the configuration file. The flowchart in Fig 2.11 illustrates the process of verification.

3. RESULTS AND DISCUSSION

As a result of this project, computation of supersonic viscous flow over air intake of McDonnel Douglas F-15 Eagle and an air intake geometry which based on air intake of scramjet, with sharp cowl leading edge were made. The aerodynamic loads on these air intake geometries were investigated under certain flight conditions. Under this title, the aerodynamic coefficient values obtained as a result of the CFD analysis made with SU2, an open-source software for two different air intake geometries, and the results obtained in the completed stages while making these calculations will be mentioned in detail. The results of flow solutions were examined using Paraview and other post processing examining methods, and decided that all results met the requirements. For this reason, the accuracy of the interpretations to be made for the results obtained has been ensured.

3.1. Verification of Geometry in First Case

In first place, for ensuring the results obtained from the flow analysis for the first case and for the accuracy of the geometry used in this case, the mass flow rate values obtained were compared with the actual flight data. The graph in the Fig 3.1 shows the momentum values which taken from the outlet of the air intake, against the length of the outlet. The momentum values were taken via Paraview by exporting the data from surface-flow.vtu file.

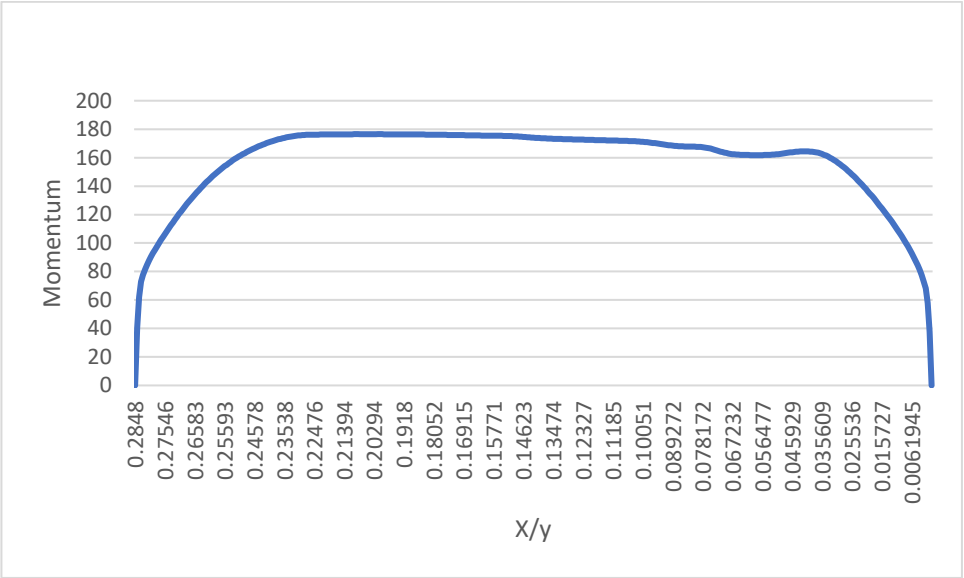

Fig 3.1 The momentum values along the outlet

By integrating this momentum values over the length of outlet, the mass flow rate values that entering the engine fan were obtained with using excel. Mass flow rate were computed as 108 kg/sec which is close to the value from the actual flight data.

The mass flow rate value taken by actual flight data is shown in the Fig 3.2.

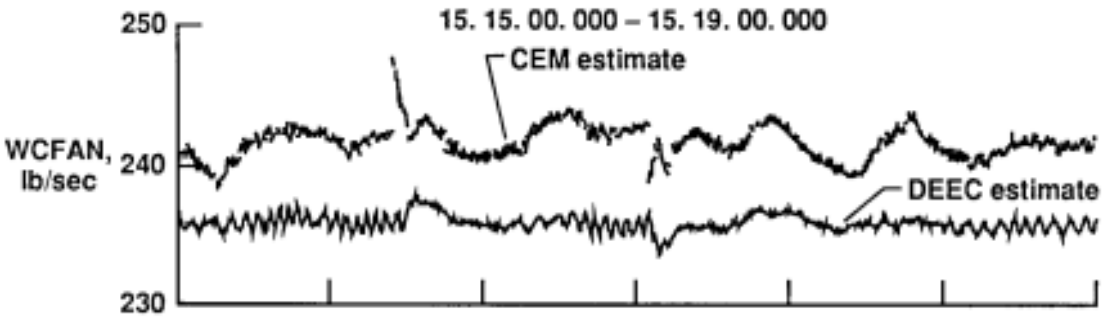

Fig 3.2 The mass flow rate throughout the engine fan in lb/sec (NASA Memorandum 4216)

3.2. Results of First Case

3.2.1. Contour Plots

The Fig 3.3 illustrates the contour plot of Mach number for flow over first air intake geometry.

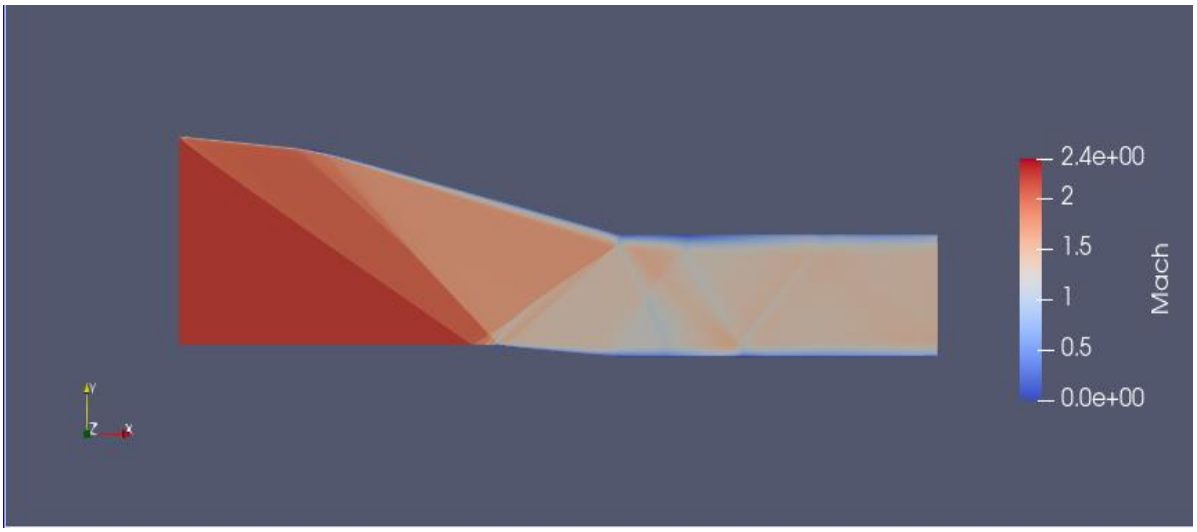

Fig 3.3 Plot of Mach number contour for flow over first geometry

As can be seen from the above Mach number contour, optimum number and location of shock waves occurred as expected. The oblique shock waves from the two external ramps intersect at the cowl leading edge, and the third oblique shock reflects upward to intersect the junction of the final ramp and the throat section. This shock system shows that proper ramp angle were selected. And it is also can be seen that these shock wave systems provide to decelerate the supersonic flow to a subsonic number and the diffuser provide further reduce the flow speed to the engine face entry speed. It is also observed that the boundary layer is formed in the regions close to the walls of the air intake. In the regions where the boundary layer is located, the velocity of the flow approaches 0. Again, from this plot of Mach number contour, the interactions of the shock waves with the boundary layer can be clearly seen. These interactions caused local thickening on the boundary layer. However, no upstream pressure gradient and backflow were observed in this flow. This is because the shock waves are not strong enough. If the multiple waves were strong enough, boundary layer thickening would increase and at some points the flow would reverse. This would cause the formation of vortexes in places. The following figures shows the plot of pressure and temperature contour for flow over first intake geometry

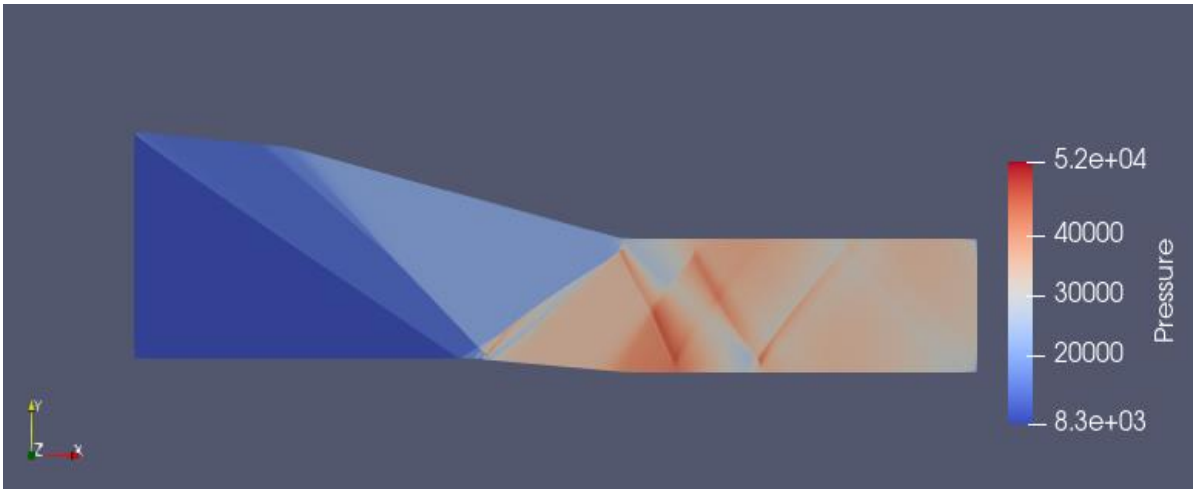

Fig 3.4 Plot of Pressure contour for flow over first geometry

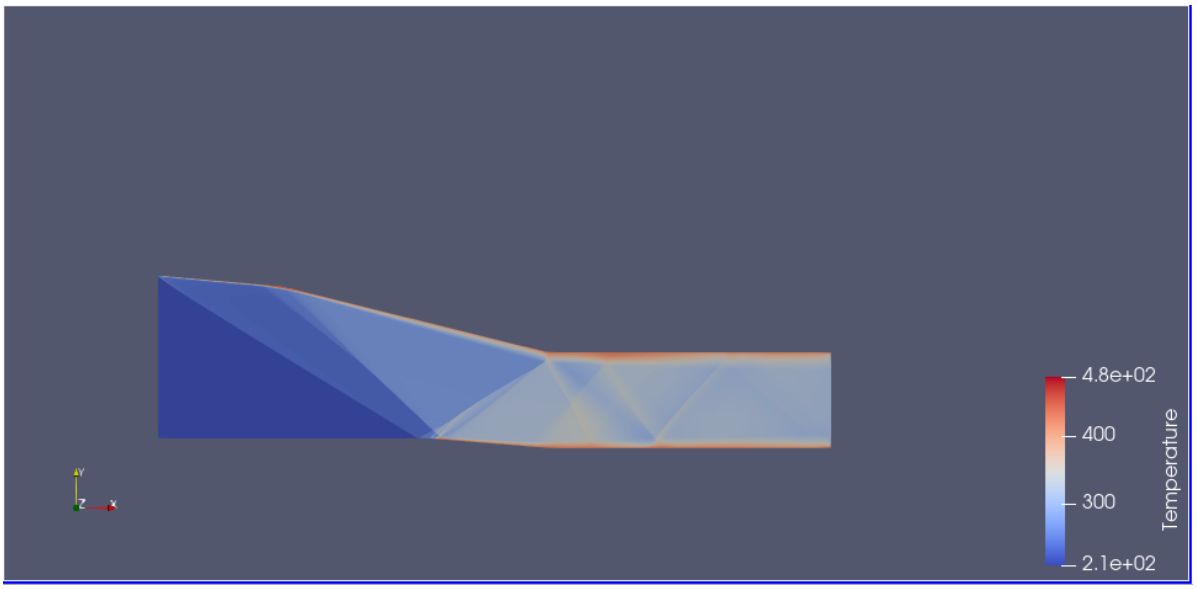

Fig 3.5 Plot of Temperature contour for flow over first geometry

As it can be seen from the Fig 3.4, as expected, increases in pressure values are observed in regions where shock waves are concentrated. Pressure increases were observed along the air intake channel as the velocity of the flow decreased due to the shock waves.

From the Fig 3.5 it is observed that due to the viscous effects of the flow, temperature increases are observed in the areas close to the wall. It is seen that the decrease in the kinetic energy of the air particles approaching 0 due to the no slip condition returns as an increase in temperature. The temperature values close to the walls reach 480 K.

3.2.2. Mach Number Values Throughout the Intake Duct

The following graph illustrates the Mach number values along the intake duct.

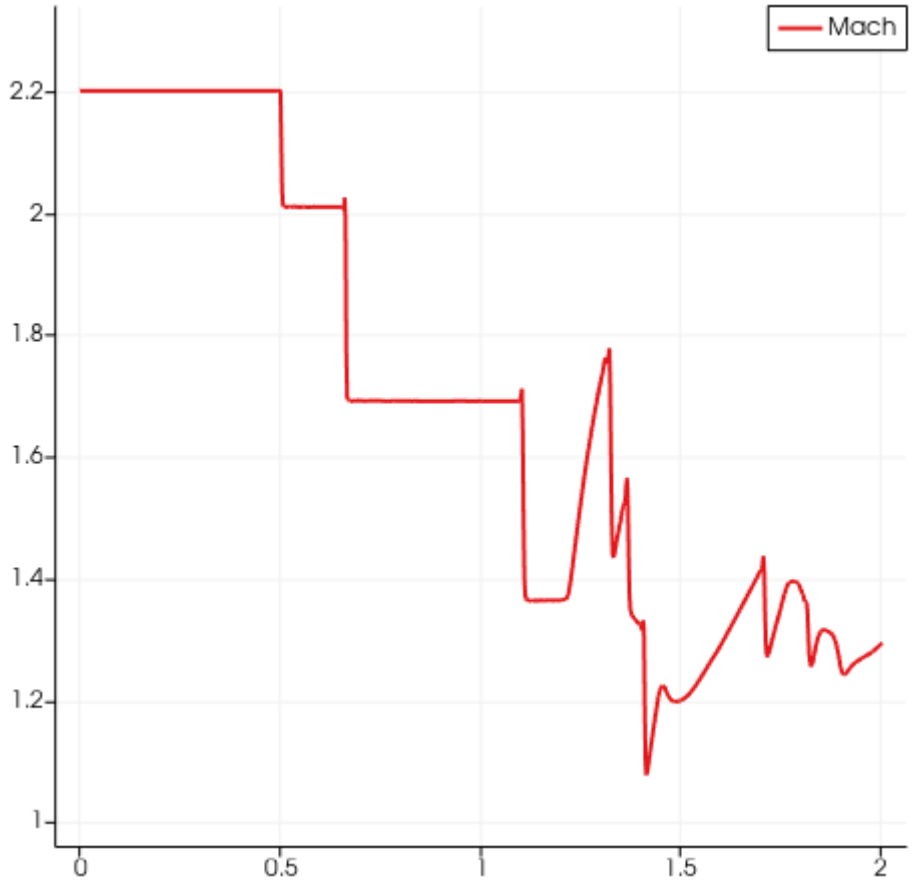

Fig 3.6 Mach Number values along the duct

It is seen that the flow Mach number values gradually decrease after each shock wave through the air intake channel. The turbulent situations seen at some points in the graph are due to the errors made in the numerical part of the flow analysis. However, it is seen that the Mach number value is still above 1 at the air intake outlet. This is likely due to the after diffuser length not being long enough at the throat part of the air intake. However, it is seen that the Mach number and flow velocity slow down due to shock waves, and this value reaches minimum values in the throat part of the air intake channel due to the intensity and strength of the shock waves.

3.2.3. Aerodynamic Coefficients for First Case

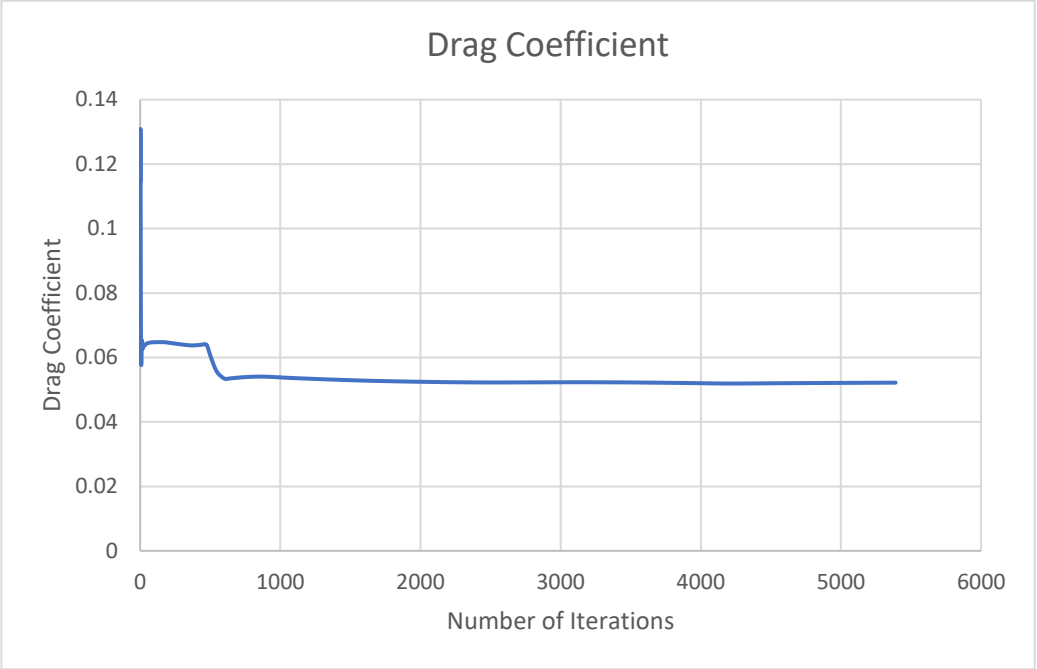

Fig 3.7 Drag coefficient against number of iteration

The fig 3.7 shows the graph of drag coefficient values during the iterations. Looking at the results obtained, we see that the drag coefficient value converged to 0.052189 and the analysis was completed.

The fig 3.8 shows the graph of lift coefficient values during the iterations.

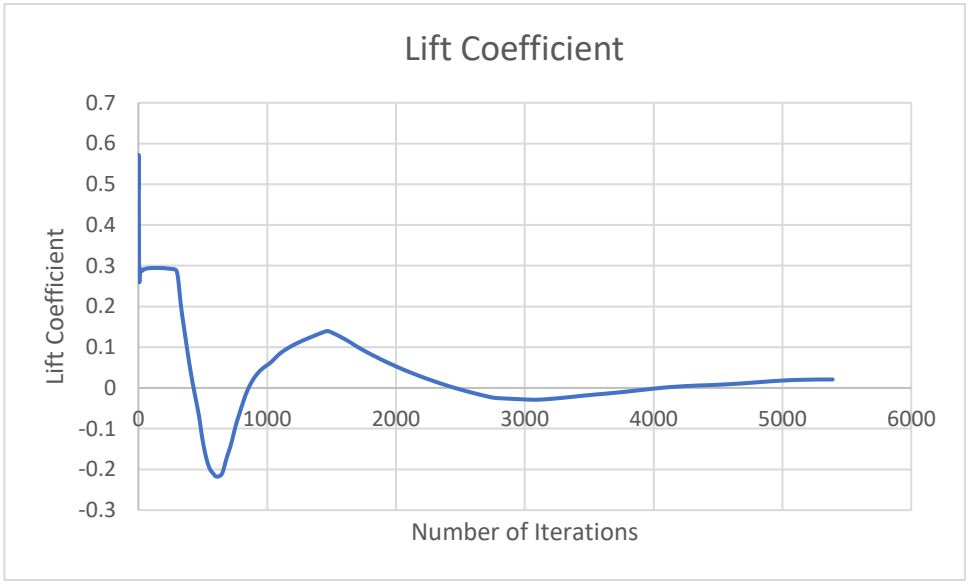

Fig 3.7 Lift coefficient against number of iteration

Looking at the results obtained, we see that the lift coefficient value converged to 0.020722 and the analysis was completed.

3.3. Results of Second Case

3.3.1. Contour Plots

The Fig 3.8 illustrates the contour plot of Mach number for flow over second air intake geometry.

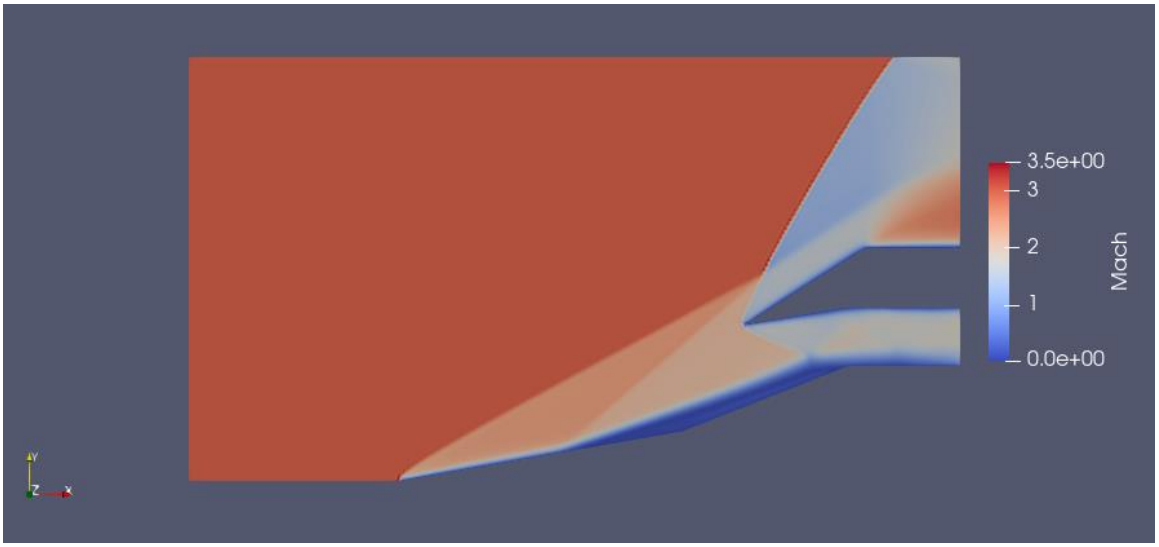

Fig 3.8 Plot of Mach number contour for flow over first geometry

As can be seen from the Mach number contour of second case geometry, again optimum number and location of shock waves occurred as expected from the referenced studies. This time the oblique shock waves from the two external ramps intersect at a little over of cowl leading edge, and then the third oblique shock reflects downward from the leading edge. When comparing with the Mach number contour from the referenced study this shock system shows that proper ramp angle were selected and accurate flow solution was made. And again it is also can be seen that these shock wave systems provide to decelerate the supersonic flow to a subsonic number and the diffuser provide further reduce the flow speed to the engine face entry speed. It is also observed that the boundary layer is formed in the regions close to the walls of the air intake. In the regions where the boundary layer is located, the velocity of the flow approaches 0. Again, from this plot of Mach number contour, the interactions of the shock waves with the boundary layer can be clearly seen. These interactions caused local thickening on the boundary layer. But this time upstream pressure gradient occurred and backflow were observed in this flow. This is because of the shock waves are strong enough and length of the ramp.

The Fig 3.9 shows the velocity vector for the flow along the duct.

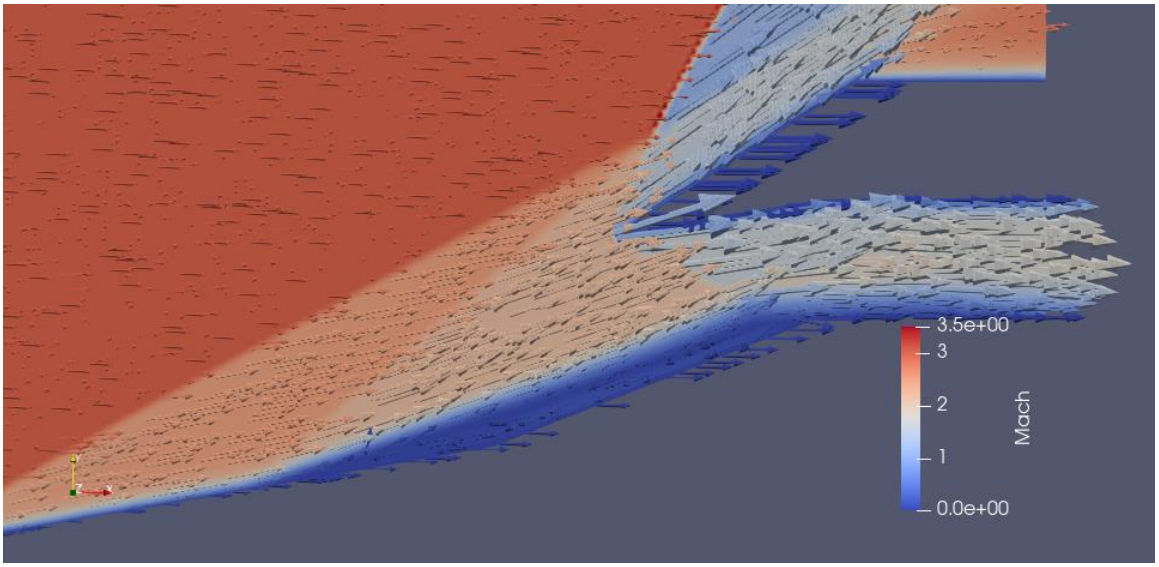

Fig 3.9 Velocity vector for flow

It is seen that in this flow due to the shock waves boundary layer thickening increase and at some points the flow is reverse. This is also cause the formation of vortexes in that field.

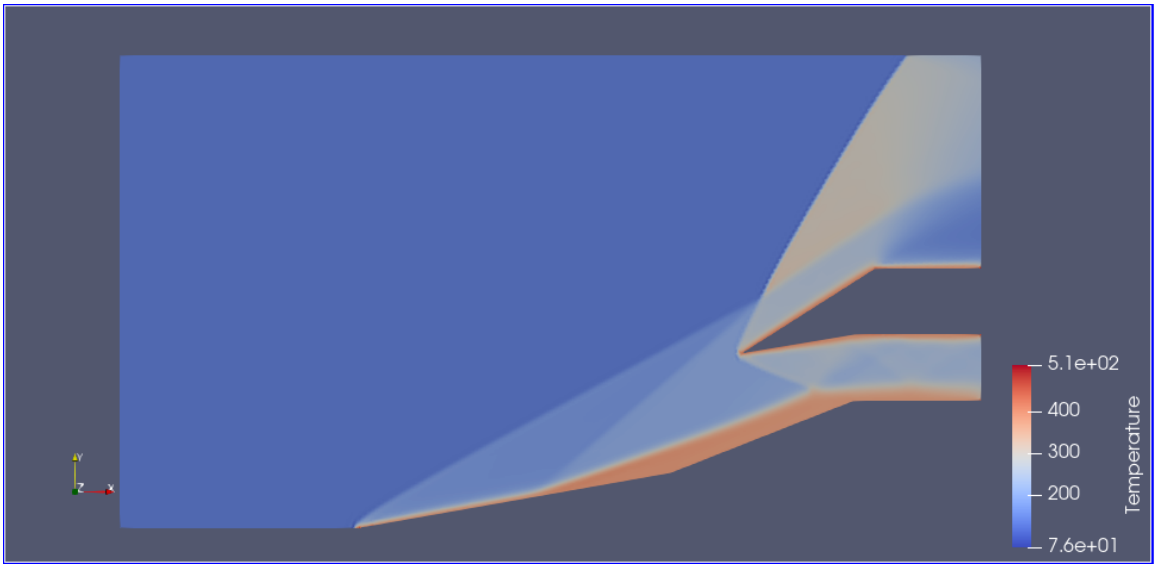

Fig 3.10 Plot of Temperature Contour for flow over second case

From the Fig 3.10 again it is observed that due to the viscous effects of the flow, temperature increases are observed in the areas close to the wall where there is no slip conditions. It is seen that the decrease in the kinetic energy of the air particles approaching 0 due to the no slip condition returns as an increase in temperature. The temperature values close to the walls reach 500 K in some areas.

3.3.2. Aerodynamic Coefficient for Second Case

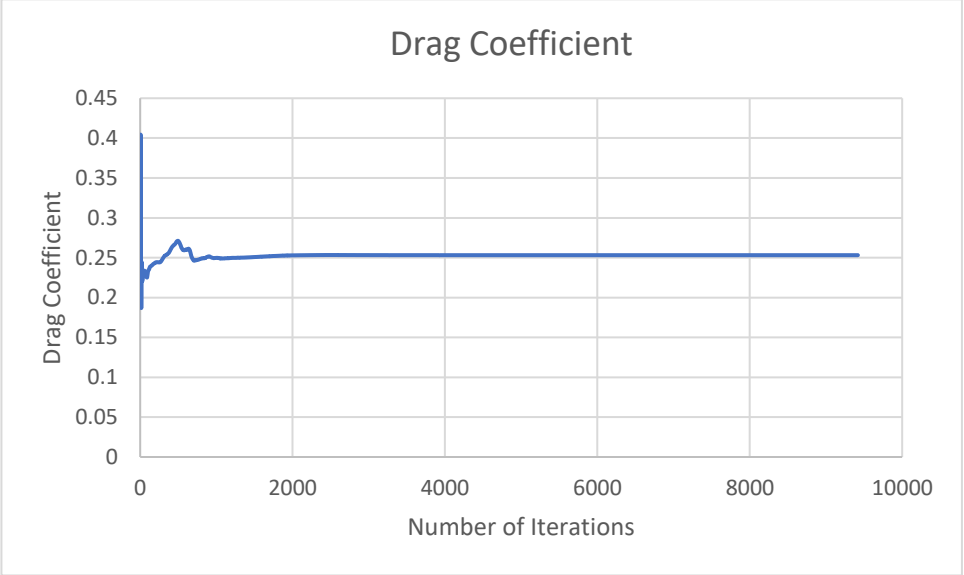

Fig 3.11 Drag Coefficient against number of iterations

The fig 3.11 shows the graph of drag coefficient values against the number of iterations. According to the results obtained, we see that the drag coefficient value converged to 0.253129 and the analysis was completed.

The fig 3.8 shows the graph of lift coefficient values during the iterations.

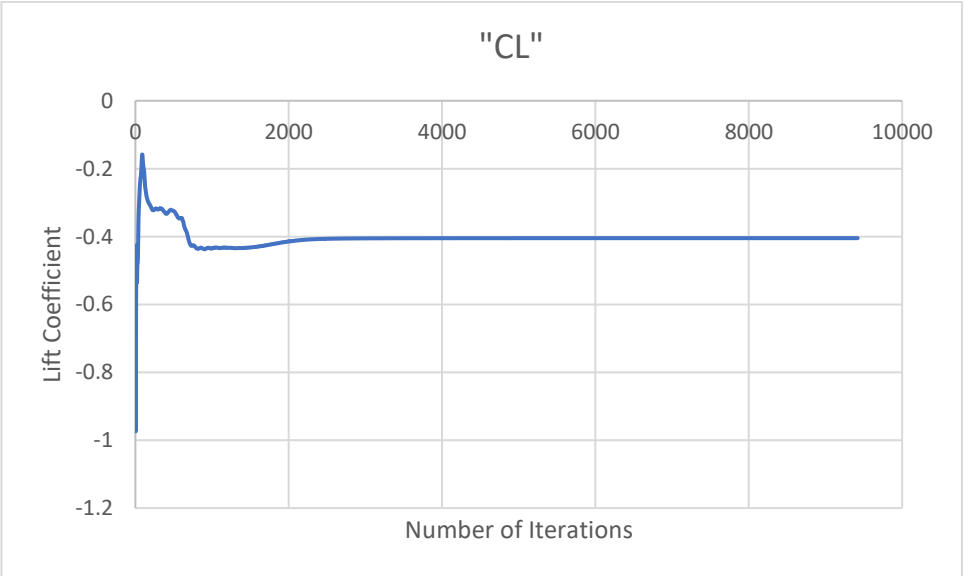

Fig 3.12 Lift Coefficient against number of iterations

According to the results from the graph, we see that the lift coefficient value converged to -0.40476 and the analysis was completed.

When the aerodynamic coefficients obtained as a result of the flow analysis for the two geometries are examined, it is seen that higher aerodynamic coefficient values are reached in the second air intake geometry. One of the reasons for this is that the flow analysis in the 2nd case is much faster than the flow analysis in the 1st case. Another reason is that as a result of the flow analysis for the 2nd air intake geometry, boundary layer thickening was encountered. These boundary layer thickenings caused reverse flow in places along the air intake surface. These reverse flows caused increases in aerodynamic coefficients.

4. CONCLUSION AND RECOMMENDATIONS

As a conclusion, air intake design and analysis processes are vital for the efficiency and healthy operation of jet engines traveling at supersonic speeds. Today the CFD method has become more applicable and widespread for the analysis and resolution of such situations and design. CFD method for flow analysis also offer much less costly and practical solutions than experimental methods. In this project of aerodynamic loads for the two different air intake geometry of supersonic aircraft were computed. Thanks to the results obtained, the size of shock waves and their interactions with the boundary layer were investigated. The aerodynamic loads occurring in the air vents due to this interaction were calculated. In a viscous flow, the behavior of the flow is observed in the regions close to the boundary layer. The types of shock waves and their effects on parameters such as temperature, pressure and velocity of the flow were observed. The analysis was optimized by considering the mass flow rate value of the selected air intake geometries for use in flow analysis. The effects of shock waves and geometry on aerodynamic loads were investigated. Increases in aerodynamic loads were studied when the boundary layer thickens, when counterflow occurs, or when strong shock waves occur. Considering the aerodynamic loads in an air intake design, how important it is on parameters such as the execution of the design, engine efficiency, pressure recovery and engine thrust value has been examined. In order to increase the efficiency of the engine and increase the pressure recovery by minimizing the aerodynamic loads on the air intake, the shock waves that will occur in the air intake should occur in optimum positions and numbers. Efficiency can be increased by slowing down the flow at an optimum level with a normal shock wave that follows a series of oblique shocks and occurs at the throat of the air intake. The analyzes and results obtained during all these processes were verified to get more accurate results.

Situations, setbacks and experiences during this project have enabled me to increase my knowledge and experience in the field of CFD many times and to familiarized with open source software such as SU2 and GMSH. In addition to these, in the field of fluids, many different gains that were not acquired at undergraduate level such as the nature of supersonic and viscous flow, shock waves occurring in flows at these speeds, boundary layer and shock wave boundary layer interactions were acquired. These achievements have been a step taken in the fields of fluids and CFD, where I plan to develop myself more with other projects planned to be realized in the future.

4.1. Experienced Problems

- The fact that the open-source software used for flow analysis during the project did not have a user-friendly interface caused a challenging process in the early stages of the project. Many problems were encountered when using GMSH during Mesh generation until getting used to with .geo coding language.
- In case 1, the dimensions of the geometry of the F-15 eagle which chosen for flow analysis could not be reached anywhere. Designing proper geometry to obtain optimum shock wave, was a challenging process.
- When I started analyzes for viscous and supersonic flow in SU2, I ran into the problem of analysis divergence. Later, I solved this problem by lowering the multi grid level value to 0.

REFERENCES

[1] Hongjun Ran and Dimitri Mavris-AIAA 2005-7357 (2005). Preliminary Design of a 2D Supersonic Inlet to Maximize Total Pressure Recovery.

[2] Trindel A. Maine, Glenn B. Gilyard, and Heather H. Lambert (August 1990). A Preliminary Evaluation of F100 Engine Parameter Estimation Process Using Flight Data. NASA Technical Memorandum 4216

[3] Bert Kinzey (1984). F-15 Eagle in detail&scale. Airlife Publishing Ltd. Tab Books inc. 20-25.

[4] J. C. Esterhuyse (March 1997). Aerodynamic Drag of a Two-Dimensional External Compression Inlet at Supersonic Speed.

[5] Fluid Dynamics Panel Working Group 13. (1991) Air Intakes for High-Speed Vehicles. AGARD Advisory Report 270, retrieved from: https://apps.dtic.mil/sti/pdfs/ADA248270.pdf

[6] P. D. Bravo - Mosquera, Aeronaves - D. Cerón - Muñoz, Aeronaves - F. Catalano, Aeronaves (2016). ANALYTICAL AND NUMERICAL DESIGN OF AMIXED-COMPRESSION AIR INTAKE FOR A SUPERSONIC FIGHTERAIRCRAFT.

[7] (B. John and P. Senthilkumar (Alterations of Cowl Lip for the Improvement of Supersonic-Intake Performance) Journal of Applied Fluid Mechanics, Vol. 11, No. 1, pp. 31-41, 2018.

APPENDICES

App. A: Fundamental SU2 Fluid Solver Configuration File

```
%%%%%%%%%%%%%%%%%%%%%%%%%%%%%%%%%%%%%%%%%%%%%%%%%%
% SU2 configuration file                                                    %
% Case description: Supersonic Viscous Flow Over Air Intake                 %
% Author: Barış BIÇAKÇI                                                     %
% Supervisor: Prof. Dr. Emre ALPMAN                                         %
% Institution: Marmara University                                           %
% Date: 2022.02.12                                                          %
% File Version 7.1.1                                                        %
%%%%%%%%%%%%%%%%%%%%%%%%%%%%%%%%%%%%%%%%%%%%%%%%%%
% ------------- DIRECT, ADJOINT, AND LINEARIZED PROBLEM DEFINITION ------------%
%
% Physical governing equations (EULER, NAVIER_STOKES,
%                  WAVE_EQUATION, HEAT_EQUATION, FEM_ELASTICITY,
%                  POISSON_EQUATION)
SOLVER= RANS
% Specify turbulence model (NONE, SA, SA_NEG, SST, SA_E, SA_COMP, SA_E_COMP, SST_SUST)
KIND_TURB_MODEL= SA
% Mathematical problem (DIRECT, CONTINUOUS_ADJOINT)
MATH_PROBLEM= DIRECT
% Restart solution (NO, YES)
RESTART_SOL= NO
% System of measurements (SI, US)
% International system of units (SI): ( meters, kilograms, Kelvins,
%                        Newtons = kg m/s^2, Pascals = N/m^2,
%                        Density = kg/m^3, Speed = m/s,
%                        Equiv. Area = m^2 )
% United States customary units (US): ( inches, slug, Rankines, lbf = slug ft/s^2,
%                        psf = lbf/ft^2, Density = slug/ft^3,
%                        Speed = ft/s, Equiv. Area = ft^2 )
SYSTEM_MEASUREMENTS= SI

% ---- NONEQUILIBRIUM GAS, IDEAL GAS, POLYTROPIC, VAN DER WAALS AND PENG ROBINSON
CONSTANTS -------%
% Fluid model (STANDARD_AIR, IDEAL_GAS, VW_GAS, PR_GAS,
%        CONSTANT_DENSITY, INC_IDEAL_GAS, INC_IDEAL_GAS_POLY, MUTATIONPP,
SU2_NONEQ)
FLUID_MODEL= STANDARD_AIR
% ----------- COMPRESSIBLE AND INCOMPRESSIBLE FREE-STREAM DEFINITION ----------%
% Mach number (non-dimensional, based on the free-stream values)
MACH_NUMBER= 2.2
% Init option to choose between Reynolds (default) or thermodynamics quantities
% for initializing the solution (REYNOLDS, TD_CONDITIONS)
INIT_OPTION= TD_CONDITIONS
% Reynolds number (non-dimensional, based on the free-stream values)
REYNOLDS_NUMBER= 6941943
% Reynolds length (1 m by default)
REYNOLDS_LENGTH= 1.0
% Angle of attack (degrees)
AOA= 0
% Side-slip angle (degrees)
SIDESLIP_ANGLE= 0.0
% Free-stream pressure (101325.0 N/m^2 by default, only Euler flows)
FREESTREAM_PRESSURE= 9183.82
% Free-stream temperature (288.15 K by default)
FREESTREAM_TEMPERATURE= 216.667

% --------------------------- VISCOSITY MODEL ---------------------------------%
% Viscosity model (SUTHERLAND, CONSTANT_VISCOSITY).
VISCOSITY_MODEL= SUTHERLAND
% Sutherland Viscosity Ref (1.716E-5 default value for AIR SI)
MU_REF= 1.716E-5
```

```
% Sutherland Temperature Ref (273.15 K default value for AIR SI)
MU_T_REF= 273.15
% Sutherland constant (110.4 default value for AIR SI)
SUTHERLAND_CONSTANT= 110.4
% ---------------------- REFERENCE VALUE DEFINITION ---------------------------%
% Reference origin for moment computation
REF_ORIGIN_MOMENT_X = 0.25
REF_ORIGIN_MOMENT_Y = 0.00
REF_ORIGIN_MOMENT_Z = 0.00
% Reference length for pitching, rolling, and yawing non-dimensional moment
REF_LENGTH= 1.0
% Reference area for force coefficients (0 implies automatic calculation)
REF_AREA= 0
% -------------------- BOUNDARY CONDITION DEFINITION -------------------------%
% Navier-Stokes (no-slip), constant heat flux wall  marker(s) (NONE = no marker)
% Format: ( marker name, constant heat flux (J/m^2), ... )
MARKER_HEATFLUX= ( UpperWall, 0, LowerWall, 0 )
MARKER_SYM = ( Symmetry )
% Supersonic inlet boundary marker(s) (NONE = no marker)
% Total Conditions: (inlet marker, temperature, static pressure, velocity_x,
%          velocity_y, velocity_z, ... ), i.e. all variables specified.
MARKER_SUPERSONIC_INLET= ( Inlet, 216.667, 9183.82, 649.5, 0.0, 0.0 )
% Outlet boundary marker(s) (NONE = no marker)
% Format: ( outlet marker, back pressure (static), ... )
MARKER_OUTLET= ( Outlet, 5000 )
% Marker(s) of the surface to be plotted or designed
MARKER_PLOTTING= ( UpperWall, LowerWall )
% Marker(s) of the surface where the functional (Cd, Cl, etc.) will be evaluated
MARKER_MONITORING= ( UpperWall, LowerWall )
% ------------ COMMON PARAMETERS DEFINING THE NUMERICAL METHOD ---------------%
%
% Numerical method for spatial gradients (GREEN_GAUSS, LEAST_SQUARES,
%                                         WEIGHTED_LEAST_SQUARES)
NUM_METHOD_GRAD= GREEN_GAUSS
% Courant-Friedrichs-Lewy condition of the finest grid
CFL_NUMBER= 5.0
% Adaptive CFL number (NO, YES)
CFL_ADAPT= NO
% Parameters of the adaptive CFL number (factor down, factor up, CFL min value,
%                                        CFL max value )
CFL_ADAPT_PARAM= ( 0.1, 2.0, 5.0, 1e10 )
% Runge-Kutta alpha coefficients
RK_ALPHA_COEFF= ( 0.66667, 0.66667, 1.000000 )
% Number of total iterations
ITER= 100000
% Linear solver for the implicit formulation (BCGSTAB, FGMRES)
LINEAR_SOLVER= FGMRES
% Preconditioner of the Krylov linear solver (ILU, JACOBI, LINELET, LU_SGS)
LINEAR_SOLVER_PREC= ILU
% Min error of the linear solver for the implicit formulation
LINEAR_SOLVER_ERROR= 1E-6
% Max number of iterations of the linear solver for the implicit formulation
LINEAR_SOLVER_ITER= 20
% ------------------------- MULTIGRID PARAMETERS -----------------------------%
% Multi-Grid Levels (0 = no multi-grid)
MGLEVEL= 0
% Multi-grid cycle (V_CYCLE, W_CYCLE, FULLMG_CYCLE)
MGCYCLE= W_CYCLE
% Multi-grid pre-smoothing level
MG_PRE_SMOOTH= ( 1, 2, 3, 3 )
% Multi-grid post-smoothing level
MG_POST_SMOOTH= ( 0, 0, 0, 0 )
% Jacobi implicit smoothing of the correction
MG_CORRECTION_SMOOTH= ( 0, 0, 0, 0 )
% Damping factor for the residual restriction
MG_DAMP_RESTRICTION= 1.0
% Damping factor for the correction prolongation
```

```
MG_DAMP_PROLONGATION= 1.0
% ------------------- FLOW NUMERICAL METHOD DEFINITION -----------------------%
%
% Convective numerical method (JST, LAX-FRIEDRICH, CUSP, ROE, AUSM, HLLC,
%                          TURKEL_PREC, MSW)
CONV_NUM_METHOD_FLOW= AUSM
% Monotonic Upwind Scheme for Conservation Laws (TVD) in the flow equations.
%          Required for 2nd order upwind schemes (NO, YES)
MUSCL_FLOW= YES
% Slope limiter (NONE, VENKATAKRISHNAN, VENKATAKRISHNAN_WANG,
%              BARTH_JESPERSEN, VAN_ALBADA_EDGE)
SLOPE_LIMITER_FLOW= VAN_ALBADA_EDGE
% Coefficient for the limiter (smooth regions)
VENKAT_LIMITER_COEFF= 0.006
% 2nd and 4th order artificial dissipation coefficients
JST_SENSOR_COEFF= ( 0.5, 0.02 )
% Time discretization (RUNGE-KUTTA_EXPLICIT, EULER_IMPLICIT, EULER_EXPLICIT)
TIME_DISCRE_FLOW= EULER_IMPLICIT
% --------------------------- CONVERGENCE PARAMETERS --------------------------%
% Convergence criteria (CAUCHY, RESIDUAL)
CONV_FIELD= RMS_DENSITY
% Min value of the residual (log10 of the residual)
CONV_RESIDUAL_MINVAL= -6
% Start convergence criteria at iteration number
CONV_STARTITER= 10
% Number of elements to apply the criteria
CONV_CAUCHY_ELEMS= 100
% Epsilon to control the series convergence
CONV_CAUCHY_EPS= 1E-10
% ------------------- TURBULENT NUMERICAL METHOD DEFINITION ------------------%
% Convective numerical method (SCALAR_UPWIND)
CONV_NUM_METHOD_TURB= SCALAR_UPWIND
% Time discretization (EULER_IMPLICIT)
TIME_DISCRE_TURB= EULER_IMPLICIT
% Reduction factor of the CFL coefficient in the turbulence problem
CFL_REDUCTION_TURB= 1.0
% -------------------------- INPUT/OUTPUT INFORMATION -------------------------%
% Screen output
SCREEN_OUTPUT=(INNER_ITER, WALL_TIME, RMS_DENSITY, RMS_ENERGY, LIFT, DRAG)
% History output groups (use 'SU2_CFD -d <config_file>' to view list of available fields)
HISTORY_OUTPUT= (ITER, AERO_COEFF)
```